JOC The Journal of Organic Chemistry

Article

pubs.acs.org/joc

Spin-Delocalization in a Helical Open-Shell Hydrocarbon

Prince Ravat, Peter Ribar, Michel Rickhaus, Daniel Häussinger, Markus Neuburger, and Michal Juríček*

Department of Chemistry, University of Basel, St. Johanns-Ring 19, 4056 Basel, Switzerland

Supporting Information

ABSTRACT: Neutral open-shell molecules, in which spin density is delocalized through a helical conjugated backbone, hold promise as models for investigating phenomena arising from the interplay of magnetism and chirality. Apart from a handful of examples, however, the chemistry of these compounds remains largely unexplored. Here, we examine the prospect of extending spin-delocalization over a helical backbone in a model compound naphtho[3,2,1-*no*]tetraphene, the first helically chiral open-shell hydrocarbon, in which one benzene ring is fused to [5]helicene, forming a phenalenyl subunit. The unpaired electron in this molecule is delocalized over the entire helical core composed of six rings, albeit in a nonuniform fashion, unlike in phenalenyl. In the case of a monosubstituted derivative, the uneven spin-distribution results in a selective σ-dimer formation in solution, as confirmed by 2D NMR spectroscopy. In contrast, the dimerization process is suppressed entirely when four substituents are installed to sterically hinder all reactive positions. The persistent nature of the tetrasubstituted derivative allowed its characterization by EPR, UV−vis, and CD spectroscopies, validating spin-delocalization through a chiral backbone, in accord with DFT calculations. The nonuniform spin-distribution, which dictates the selectivity of the σ-dimer formation, is rationalized by evaluating the aromaticity of the resonance structures that contribute to spin-delocalization.

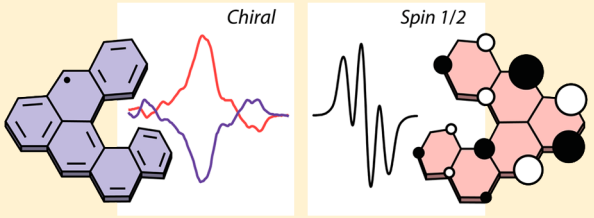

INTRODUCTION

Spin-delocalization is an intrinsic feature[1] of π-conjugated open-shell molecules that contain one or more unpaired π-electrons. A prototypical example of neutral spin-delocalized systems is phenalenyl[2] (**1**, Figure 1), a three-ring triangular hydrocarbon (HC), in which one of the 13 π-electrons is unpaired and uniformly delocalized between six positions. The spin-delocalized nature of planar systems such as **1** determines their propensity to self-assemble[3] via formation of multicenter bonds[4] and hence dictates their magnetic and conducting properties[3,5,6] in the solid state. Extending spin-delocalization through a nonplanar, helically twisted backbone brings an additional element, that of chirality, and links it in a unique manner with the properties arising from nonzero spin. Such union of spin and chirality can provide useful model systems for investigating effects arising from the interplay of magnetism and chirality, which have recently gained considerable fundamental interest as they create[7] a broad spectrum of technological opportunities. These phenomena emerge on account of the simultaneous breaking of parity and time-reversal symmetries in magnetized chiral systems, and cause nonreciprocal dependence of (1) absorption/emission of unpolarized light[8] and (2) electrical resistance[9] on the direction of magnetization.

Whereas numerous examples of planar open-shell systems based on **1** are known,[1] the chemistry of related helical HC systems remains, with an exception of two examples[10] that contain heteroatoms, unexplored. The only nonplanar HC featuring the phenalenyl subunit that has been described[11] to date is a bowl-shaped corannulene derivative **2** (Figure 1). The parent neutral radical compound could not, however, be detected and only its anionic closed-shell species were characterized. This seminal contribution was shortly followed by a report[10b] describing the first helical phenalenyl-based radical **3**, featuring a hetero-[4]helicene backbone. Compound **3** displayed spin-delocalization over the entire π-conjugated twisted path and could be resolved into its enantiomers that showed complementary CD spectra. Most recently, one more example[10a] of a nonplanar phenalenyl derivative comprising a hetero-[4]helicene backbone, compound **4**, was described. In both cases, the spin density was delocalized over the phenalenyl subunit to a greater extent compared with other rings of the π-conjugated path. This intriguing feature inspired us to investigate whether spin-delocalization can be extended over larger helical systems and what structural elements affect it.

Here, we describe the synthesis and properties of two substituted derivatives of naphto[3,2,1-*no*]tetraphene (**5a**, Figure 1), and demonstrate that spin-delocalization can be extended over a [5]helicene backbone (in red), which ensures[12] nonplanarity and inherent chirality of the system. In this helically chiral HC, the spin density is delocalized over the entire core composed of six rings, albeit in a nonuniform fashion, with the largest spin densities displayed by the peripheral carbon atoms of the phenalenyl unit, similarly to **3** and **4**. In the case of monosubstituted derivative **5b**, the nonsymmetric electronic structure results in the selective σ-dimer-formation process, as confirmed by 2D NMR spectroscopy in solution. In contrast, this dimerization process is

Received: September 12, 2016
Published: November 3, 2016

DOI: 10.1021/acs.joc.6b02246
J. Org. Chem. 2016, 81, 12303−12317

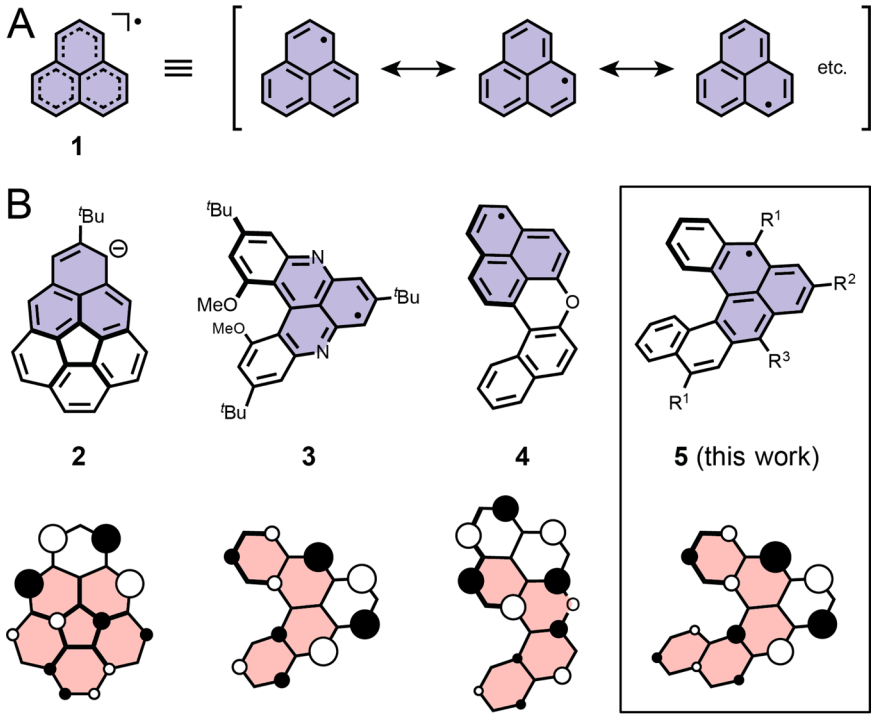

Figure 1. (A) Structural formulas of the resonance forms of phenalenyl (**1**). (B) Structural formulas and SOMOs (obtained from Hückel molecular orbital analysis) of nonplanar derivatives of **1**: bowl-shaped anion **2** (HOMO shown), hetero-[4]helicene-based radicals **3** and **4**, and [5]helicene-based radical **5** described in this work (**5a**: R^1, R^2, R^3 = H; **5b**: R^1, R^2 = H, R^3 = Ph; **5c**: R^1, R^3 = Ph, R^2 = ^{t}Bu). Color code: phenalenyl subunits/purple, corannulene and helicene subunits/red.

Scheme 1. Synthesis of Precursors 9a, 9b, and 15, and Target Compound 5c[a,b]

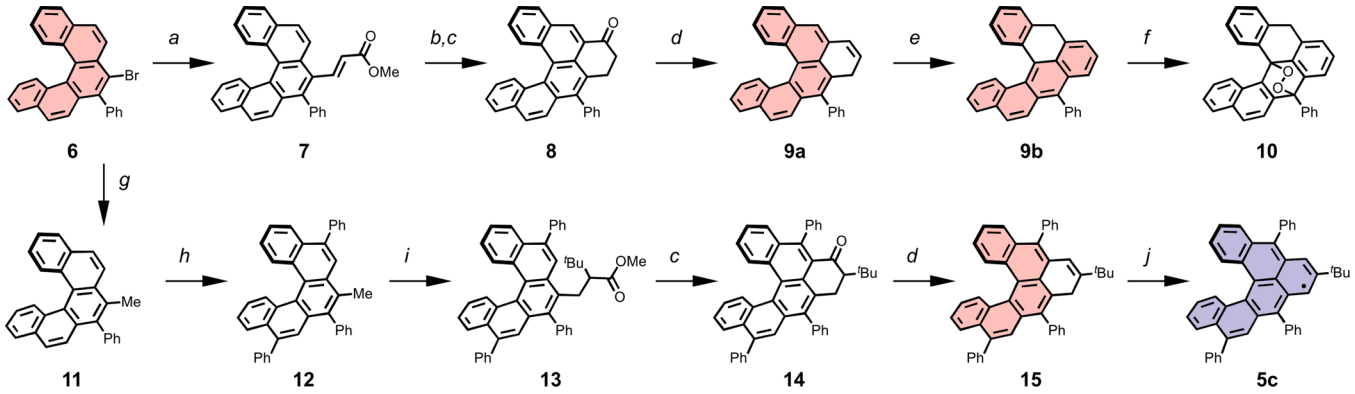

[a]Reaction conditions: (a) methyl acrylate, $Pd(OAc)_2$, PPh_3, K_2CO_3, Bu_4NBr, DMF, 110 °C, 88%; (b) H_2, Pd/C, CH_2Cl_2/EtOH, room temperature, 98%; (c) (i) LiI, 2,4,6-collidine, 185 °C, (ii) $C_2O_2Cl_2$, 65 °C, (iii) $AlCl_3$, CH_2Cl_2, −78 to −10 °C, 55% (**8**)/62% (**14**); (d) (i) $NaBH_4$, CH_2Cl_2/EtOH, room temperature, (ii) *p*-TSA, toluene, 90 °C, 64% (**9a**)/59% (**15**); (e) TFA, CH_2Cl_2, room temperature, 85%; (f) O_2, ambient light, quantitative; (g) MeMgBr, $Ni(dppp)Cl_2$, Et_2O, 0 to 45 °C, 98%; (h) (i) Br_2, CH_2Cl_2, −78 °C to room temperature, (ii) phenylboronic acid, $Pd(PPh_3)_4$, K_2CO_3, toluene/EtOH/H_2O, 85 °C, 86%; (i) (i) NBS, dibenzoyl peroxide, CCl_4, 87 °C, (ii) methyl 3,3-dimethylbutanoate, LDA, THF, −78 °C to room temperature, 60%; (j) *p*-chloranil, C_6H_6, 65 °C. [b]The aromatic rings of **6**, **9a**, **9b**, and **15** are highlighted in red. The open-shell core of **5c** is highlighted in purple.

suppressed in the case of tetrasubstituted derivative **5c**, on account of steric hindrance introduced around all of the reactive positions. The persistent nature of **5c** allowed its characterization by variable-temperature (VT) EPR and NMR, and UV−vis spectroscopies, MALDI-ToF spectrometry, as well as CD spectroscopy of its two enantiomers that displayed mirror-like Cotton effects in their CD spectra. In addition, we show that the *nonuniformity* of the spin-density distribution as well as the *selectivity* of the σ-dimer-formation process can be rationalized by evaluating the aromaticity of the resonance structures that contribute to spin-delocalization, and support our conclusions with the aid of DFT calculations.

RESULTS AND DISCUSSION

Synthesis. Initially, the preparation of the parent compound **5a** starting from 3-bromodibenzo[*c*,*g*]phenanthrene[13] was attempted, following a modified synthetic strategy for **5b** outlined in Scheme 1. The required keto-intermediate (an unsubstituted analogue of **8**) did not, however, form over the course of the Friedel−Crafts acylation (see Experimental

DOI: 10.1021/acs.joc.6b02246
J. Org. Chem. 2016, 81, 12303−12317

Section and Section S2 for details) and it was necessary to block the 4-position next to the bromo-substituent. Compound **6** bearing a phenyl substituent at this position was therefore employed as the starting material to successfully synthesize the mono- and tetrasubstituted derivatives of **5a** (**5b** and **5c**, respectively, Scheme 1).

Compound **9a**, the precursor of the monosubstituted derivative **5b**, was prepared in seven steps from the racemic starting material **6** (Scheme 1, top) that was obtained by the Suzuki coupling of 3,4-dibromodibenzo[*c*,*g*]phenanthrene.[13] The Heck coupling of **6**, which afforded **7** in 88% yield, was followed by reduction, demethylation, and acid chloride formation before the Friedel−Crafts acylation step, which this time yielded exclusively intermediate **8** in 54% yield over the four steps. After reduction of **8** and subsequent dehydration, the hydro-precursor **9a** was obtained in 64% yield over the two steps, as a solid material that in the presence of an acid isomerizes to its more stable isomer **9b**.

This isomerization process occurs spontaneously in deuterated solvents that contain trace amounts of acids, such as CD_2Cl_2, during an NMR experiment (see Figure S1), or it can be performed on a larger scale by using trifluoroacetic acid, which instantly converts **9a** to **9b** that can be purified by column chromatography and isolated. The observed isomerization process is in accord with the results from DFT calculations at the B3LYP/6-31G(d,p) level of theory, which predict that **9b** is lower in energy compared to **9a** by 4.6 kcal mol^{-1}. This energy difference is most likely the result of either (1) different strain energies, as the calculated distance between two "fjord" hydrogen atoms, 1-H and 15-H (see Figure 3B), is 2.7 Å in **9a** and 2.9 Å in **9b**, (2) different degrees of aromaticity, as all 24 π-electrons of **9b** are part of either a six-π-e^- or an 18-π-e^- aromatic system, while two π-electrons of **9a** form a double bond that is conjugated to a 22-π-e^- aromatic system (highlighted in red in Scheme 1), or (3) the combination of the two effects.

It is of interest to note that while **9b** is stable in the dark or in the absence of oxygen, it undergoes a clean transformation to form endoperoxide **10** in the presence of oxygen and ambient light at room temperature (Scheme 1). Such a reaction is not unusual, and it has been observed[14] previously for analogous systems containing a twisted tetraphene moiety. The driving force of this transformation, or at least a part of it, seems to be the release of strain energy upon formation of the 2,3-dioxabicyclo[2.2.2]octane subunit during this reaction. The strain release is reflected by the change in the chemical shift of proton 15-H (8.90 ppm in **9b** and 7.14 ppm in **10**) in the fjord region of the [5]helicene unit, when the distance between protons 1-H and 15-H is increased from 2.9 Å in **9b** to 3.1 Å in **10** (DFT/B3LYP/6-31G(d,p)).

The precursor of the tetrasubstituted derivative **5c**, compound **15**, was prepared in ten steps from the racemic starting material **6** (Scheme 1, bottom). In this case, the synthetic strategy was slightly altered, as two additional phenyl substituents had to be introduced in **11** that was obtained by the Kumada coupling of **6** in 98% yield. The two phenyl groups were installed by a selective bromination of **11** followed by the Suzuki coupling to afford intermediate **12**, bearing three phenyl and one methyl substituents, in 86% yield. The methyl group of **12** was brominated with NBS and then reacted with a lithium salt of methyl 3,3-dimethylbutanoate to afford **13** in 60% yield over the two steps. To build the remaining six-membered ring, the same reaction sequence as for **8**, namely, demethylation, acyl chloride formation, and the Friedel−Crafts acylation, was employed to form intermediate **14** in 62% yield over the three steps. The subsequent reduction and dehydration yielded the hydro-precursor **15**, bearing three phenyl and one *tert*-butyl substituents, in 59% yield over the two steps. In contrast to **9a**, compound **15** does not isomerize in CD_2Cl_2, either because **15** represents the most stable isomer or the energy barrier for the isomerization process is higher than that for **9a**.

All compounds were characterized by ^1H and ^{13}C NMR spectroscopy, and MALDI-ToF mass spectrometry. The key intermediates and the hydro-precursors **9a**, **9b**, and **15**, as well as the endoperoxide **10** were additionally characterized by 2D NMR spectroscopic techniques (COSY, NOESY, HMQC, and HMBC), which allowed a full assignment of their ^1H and ^{13}C resonances to the corresponding hydrogen and carbon atoms, respectively (see the SI). The structure of **15** was additionally confirmed by a single-crystal X-ray diffraction analysis (Figure 2). The target compounds **5b** and **5c** were generated in situ from the hydro-precursors **9** and **15** by using oxidant *p*-chloranil in argon-saturated benzene or toluene, and their properties are discussed below.

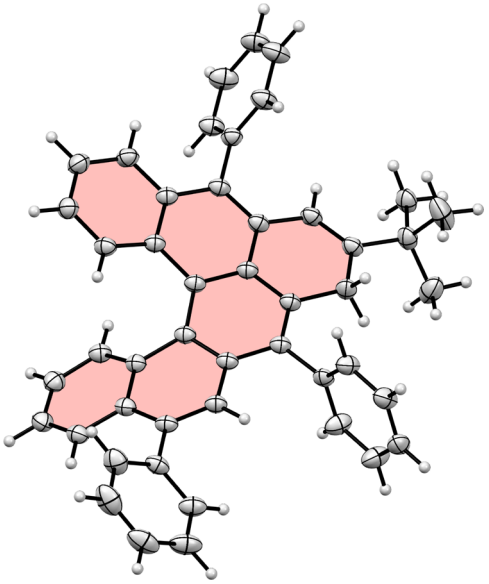

Figure 2. Solid-state structure of hydro-precursor **15** obtained by single-crystal X-ray diffraction analysis. The thermal ellipsoids are shown at a 50% probability level.

DFT Analysis. The DFT calculations at the UB3LYP/6-31G(d,p) level of theory were performed on the parent compound **5a** to gain insight into the electronic structure of the target molecules (Figure 3A). These results show that the distribution of the singly occupied (SOMO) and the lowest unoccupied (LUMO) molecular orbitals, as well as the spin density of **5a** are largely delocalized over the entire helically twisted backbone. In contrast to phenalenyl (Figure 3A, top), where the spin density is distributed uniformly, however, **5a** displays (Figure 3A, bottom) a nonuniform spin-density distribution over the six rings. A more quantitative picture can be obtained by comparing the values of positive Mulliken spin densities of the corresponding atoms (Figure 3B, bottom right), which are distinctly higher (0.27−0.35) in the case of peripheral carbon atoms of the phenalenyl unit (positions 5, 6, 8, and 9) than those (0.05−0.12) of the remaining peripheral

DOI: 10.1021/acs.joc.6b02246
J. Org. Chem. 2016, 81, 12303−12317

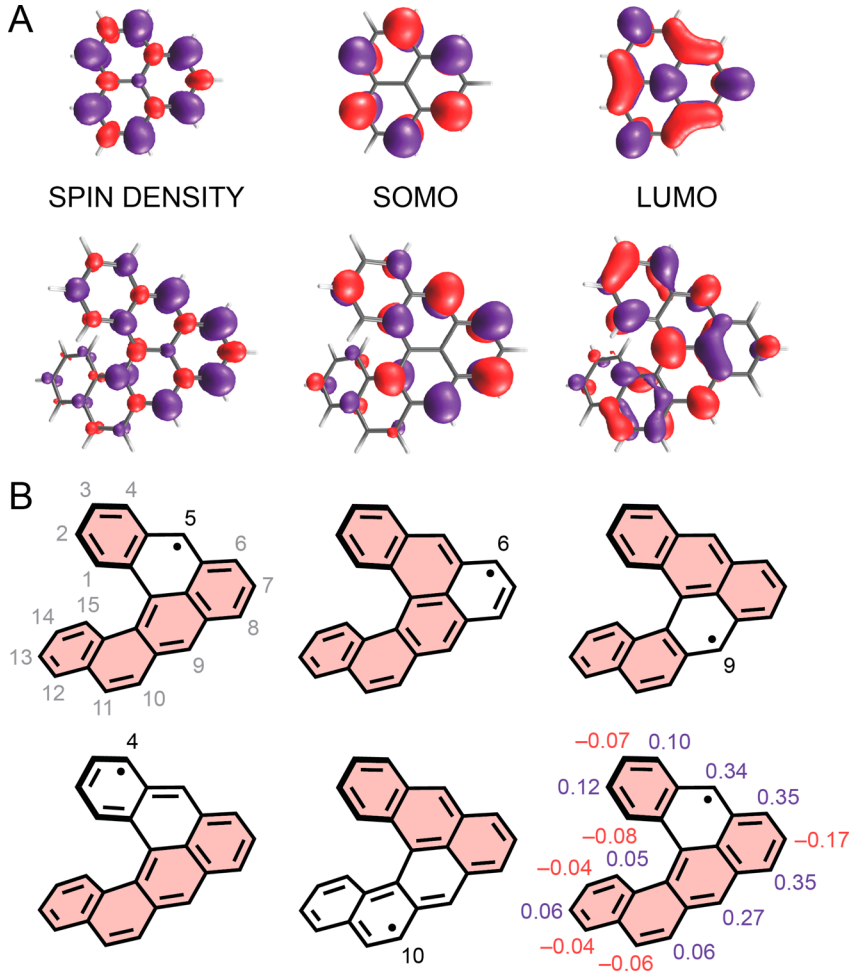

Figure 3. (A) Spin density and the singly occupied (SOMO) and the lowest unoccupied (LUMO) molecular orbitals of phenalenyl (top) and **5a** (bottom) and (B) representative examples of the resonance structures of **5a** (numbers denote the position of the unpaired electron) and Mulliken spin densities for **5a** (bottom right; positive and negative values are denoted in purple and red, respectively). The aromatic rings in the corresponding resonance structures are highlighted in red.

positions (2, 4, 10, 13, and 15) of the [5]helicene unit (for numbering, see Figure 3B, top left).

To understand and rationalize the nonuniform spin-density distribution, we evaluated the aromaticity of the resonance structures (Figure 3B) that contribute to spin-delocalization. The resonance structures with the highest degree of aromaticity, that is, structures with the highest number of aromatic rings, were assumed to be the most stable ones and thus contribute to spin-delocalization to a greater extent than those with a lower number of aromatic rings. Accordingly, the resonance structures with the unpaired electron at positions 5, 6, 8, and 9, which all contain the maximum number (five) of aromatic rings (highlighted in red, Figure 3B, top), contribute to spin-delocalization more than structures with the unpaired electron at positions 2 and 4 (four aromatic rings), and these contribute more than those with the unpaired electron at positions 10, 13, and 15 (three aromatic rings, Figure 3B, bottom).

This evaluation is in a good qualitative agreement with the positive Mulliken spin densities obtained from DFT calculations (Table S1), which provide values 0.27−0.35 for positions 5, 6, 8, and 9, 0.10−0.12 for positions 2 and 4, and 0.05−0.06 for positions 10, 13, and 15, and can be carried out in a similar fashion also for the nonperipheral positions. This analysis is further supported by the NICS(1) values obtained by the GIAO-UB3LYP/6-31G(d,p) calculations (Table S2), which show that the two outer rings of the [5]helicene unit possess a higher degree of aromatic character than the remaining [5]helicene rings, and the ring that is not part of the [5]helicene unit displays the lowest degree. The same exercise can be carried out to rationalize the nonuniform spin-density distribution of **3** and **4** (Figure 1), and applied to other spin-delocalized structures in general.

Properties of 5b. First, we investigated the effect of the nonuniform spin-delocalized electronic structure of **5a** on the σ-dimer-formation process of its monosubstituted derivative **5b**. Compound **5b** was generated in situ, by oxidation of either **9a** or **9b** with *p*-chloranil (CA) in argon-saturated solvents at room temperature (Figure 4), and the reaction was monitored by EPR (toluene) and NMR (C_6D_6) spectroscopy in solution. Two hours after the addition of two equivalents of CA to **9a**, a very weak unresolved signal that diminished within a few hours was observed in the EPR spectrum (Figure S18). When the same reaction was followed (Figure 4) by ^{1}H NMR spectroscopy, all major components that formed over the course of the reaction could be unambiguously identified (Section S3) with the help of high-resolution 2D NMR techniques, HSQC and HMBC. Within 3 h after the addition of

DOI: 10.1021/acs.joc.6b02246
J. Org. Chem. 2016, 81, 12303−12317

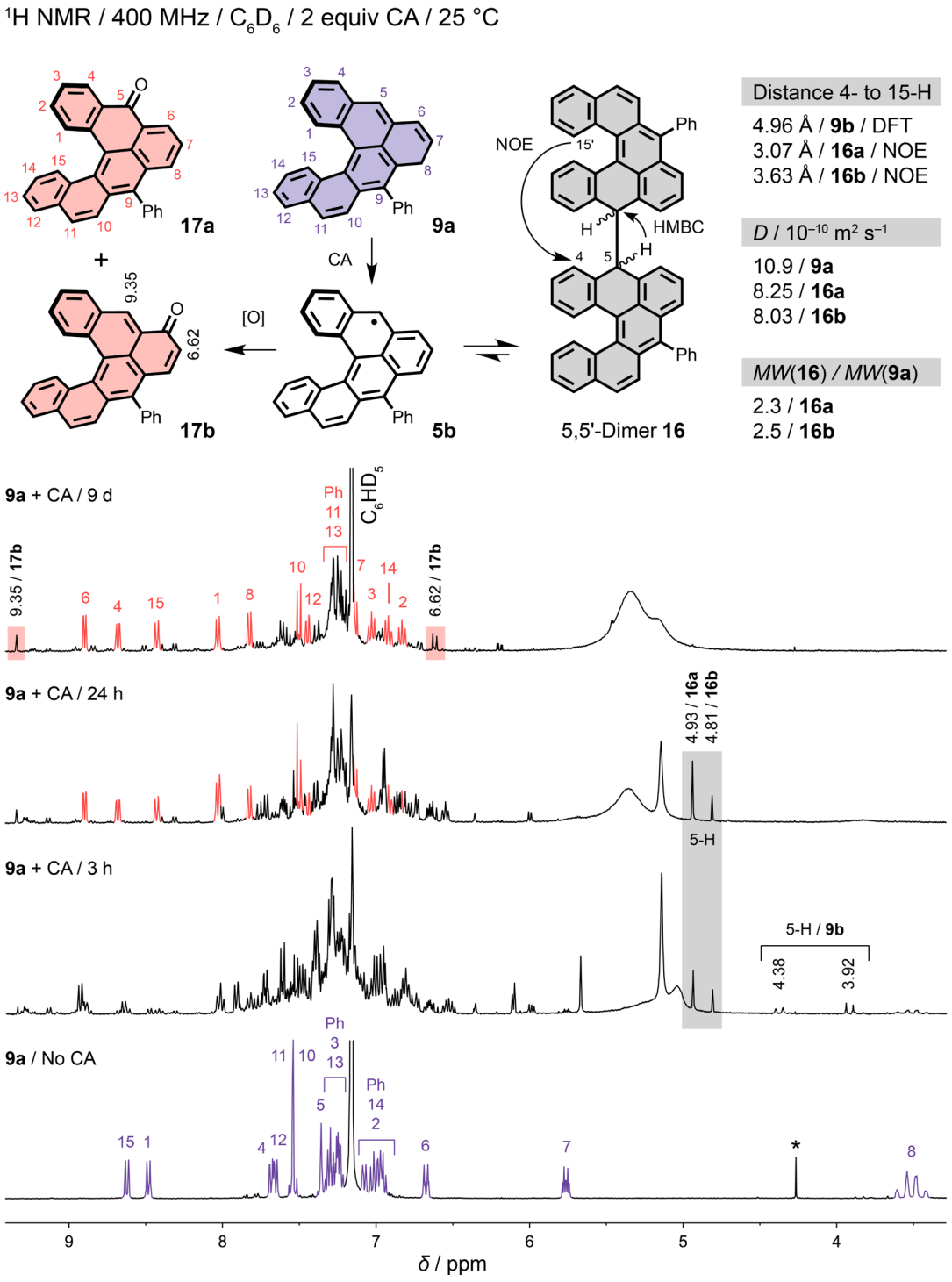

Figure 4. ^{1}H NMR Spectra (400 MHz, C_6D_6, 25 °C) recorded before and after the addition of two equivalents of *p*-chloranil (CA) to **9a**, which generates radical species **5b** that are in equilibrium with *σ*-dimers **16** and undergo slow oxidation to the final species **17**. Assignment of the signals corresponding to **9a** (purple) and **17a** (red) is shown. The signals at 9.35 and 6.62 ppm (red) correspond to **17b** and the signals at 4.93 and 4.81 ppm (gray) correspond to **16a** and **16b**, respectively. Partial isomerization of **9a** to **9b** was observed. The signals at ∼5.0−5.5 ppm that broaden as the reaction progresses belong to reduced CA species. *D* = diffusion coefficient, MW = molecular weight, * = residual CH_2Cl_2.

CA, the starting material **9a** was almost completely consumed and proton resonances of new species appeared, including two singlets at 4.93 and 4.81 ppm. These species were identified as two 5,5′-*σ*-dimers of **5b** (**16a** and **16b**), most likely diastereomers, which are in dynamic equilibrium with the monomeric species **5b**. The observed sharp well-resolved ^{1}H NMR signals and the weak EPR signal indicate that this equilibrium is shifted strongly in favor of the *σ*-dimers **16**. Within 24 h, proton resonances of two additional species were detected and assigned to compounds **17a** and **17b**, products of oxidation of **5b** bearing an oxo group at the 5- and 6-position, respectively. Presumably, the oxidation of **5b** occurs on account of trace amounts of oxygen present in the argon-saturated sample and results in slow conversion of the reaction mixture to

DOI: 10.1021/acs.joc.6b02246
J. Org. Chem. 2016, 81, 12303−12317

the mixture of almost exclusively **17a** and **17b** over a few days (Figure 4), which is in accord with the disappearance of the signal during an EPR experiment. This final mixture is stable for at least 40 days at room temperature in a sealed tube.

The structures of compounds **17a** and **17b** were unequivocally confirmed by 2D NMR spectroscopy of the final mixture, while the structures of **16a** and **16b** were validated during a separate NMR experiment at a lower temperature (15 °C; Figures S12−S15), where these species displayed a prolonged lifetime of approximately 1 day.

The structures of **16a** and **16b** were verified based on the following proofs (Figure 4 and Section S3): (1) The monomeric unit of both **16a** and **16b** features an sp^3 carbon atom at the 5-position, as confirmed by 2D NMR techniques. The observed chemical shifts of the signals at 4.93 and 4.81 ppm that belong to the protons of sp^3 carbon atoms of **16a** and **16b**, respectively, are in agreement[15] with the shifts of analogous σ-dimers. (2) The proton resonances at 4.93 and 4.81 ppm show an HMBC correlation with the carbon resonances at 58.3 and 58.2 ppm, respectively, which belong to the sp^3 carbon atoms at the 5-position. Such correlation is only possible in the case of a 5,5′-σ-dimer comprising two identical monomeric units. (3) Using the 1-H/15-H NOESY signal as a standard, assuming that the distance between 1-H and 15-H is roughly 2.87 Å (a value obtained by DFT for **9b**), a 4-H/15-H distance of 3.07 Å (**16a**) and 3.63 Å (**16b**) was estimated by integration of the corresponding NOESY signals. These distances are significantly shorter than the calculated 4-H/15-H distance (4.96 Å) in **9b**, which indicates that the observed NOESY signals correspond to the 4-H/15′-H correlations between, and not within, the monomeric units, in accord with the dimeric structure of **16**. (4) The molecular weight ratios of **16a** (2.3) and **16b** (2.5) to **9a**, estimated from the diffusion coefficients (D) obtained by PFGSE NMR spectroscopy, further support the dimeric structure of **16**. Almost identical results were obtained when **9b** was used as the starting material, as its oxidation with CA generates the same species **5b** as when compound **9a** is used.

The observation of exclusively the 5,5′-σ-dimer species **16** during the ^{1}H NMR experiments indicates that the σ-dimer-formation process of **5b** is regioselective, which is in accord with the nonuniform profile of spin-distribution in **5b** (Table S1). On the basis of the values of positive Mulliken spin densities and excluding the 8-, 9-, and 10-positions, which are sterically hindered by a phenyl substituent at the 9-position, the 5- and 6-positions are expected to be favored over the remaining unhindered positions in the dimerization process. Although the 5- and 6-positions display similar values of positive Mulliken spin densities, the 5−5′-connection mode is favored over the 6−6′ or 5−6′ modes, based on the results from the ^{1}H NMR spectroscopy. The σ-dimers possess four stereogenic elements (two centers and two axes) and therefore exist in the form of multiple stereoisomers. In the case of 5,5′-σ-dimer, for example, six diastereomers are possible. Additionally, each stereoisomer can possibly form several stable conformations. Consequently, the regioselectivity observed for the dimerization of **9b** is likely the result of an interplay between the kinetic and thermodynamic parameters associated with this process that allows observation of two 5,5′-σ-dimer species **16a** and **16b** in the NMR time scale.

The nonuniform spin-distribution in **5b** also affects the selectivity of the oxidation reaction, which occurred at the 5- and 6-positions, as confirmed by ^{1}H NMR spectroscopy, affording **17a** and **17b** as the major final products. Again, this observation is in agreement with the spin-distribution in **5b** (Table S1), which makes the 5- and 6-positions more prone toward oxidation than the other positions. The formation of compound **17a** was favored over its isomer **17b** and according to DFT calculations (DFT/B3LYP/6-31G(d,p)), **17a** is lower in energy by 2.9 kcal mol^{-1} compared with **17b**, similarly to the case of **9a** and **9b**.

Properties of 5c. To increase the kinetic stability of **5b**, three additional substituents were introduced in the tetrasubstituted derivative **5c**, which protect all of the most reactive positions (5, 6, 8, and 9) and, consequently, suppress the σ-dimer-formation process entirely. Compound **5c** was generated from hydro-precursor **15** by using one equivalent of CA in argon-saturated solvents at 65 °C, and proved to be stable under argon-saturated conditions at room temperature and in the presence of light. The persistent nature allowed its characterization by variable-temperature (VT) EPR and UV−vis spectroscopy, as well as MALDI-ToF mass spectrometry (SI, page S104).

The formation of **5c** was first monitored by ^{1}H NMR spectroscopy in C_6D_6 at 65 °C, which showed almost complete disappearance of the resonances corresponding to the starting material **15** within 3 h after the addition of CA. No new resonances appeared during this period, and no signals could be detected even when the sample was cooled to 200 K (toluene-d_8), indicating that the σ-dimer-formation was indeed suppressed. An argon-saturated sample of freshly generated **5c** in toluene was subsequently studied by EPR spectroscopy (Figure 5). At room temperature, the sample exhibited a three-broad-line EPR spectrum at a g-value of 2.0036, which is in accord with spin-1/2 hydrocarbons. The two observed proton hyperfine coupling constants (a_1 and a_2) were roughly 7.0 and 7.1 G (Figure 5B).

The proton hyperfine coupling constant, a_H, values for **5c** (Figure 5A) were obtained from DFT calculations (UB3LYP/EPR-III) on the optimized geometry (UB3LYP/6-31G(d,p)) and indicate that spin-density is delocalized over the entire hydrocarbon core. The highest absolute a_H values were obtained for the hydrogen atoms of the phenalenyl moiety (7.57 and 7.02 G, purple), while the hydrogen atoms of the remaining three rings display distinctly lower absolute a_H values (0.69−2.68 G, red), following the nonuniform distribution of spin density, which is delocalized primarily over the phenalenyl core. Because of the large number of nonequivalent protons displaying similar absolute a_H values in the range 0.69−2.68 G (red), only the two highest a_H values (purple) could be elucidated from our experimental data (Figure 5A,B). The measured EPR spectrum is, however, in a good agreement with the simulated spectrum (Figure S19) obtained by using the calculated a_H values. In addition, the VT-EPR spectra were recorded for **5c** at two different spin concentrations (1.3×10^{-4} and 1.5×10^{-5} M, calibrated with TEMPO) in toluene. In both cases, the EPR signal intensity increased upon decreasing the temperature, in accord with the Curie law (Figure 5C), which further supports[15,16] that **5c** does not undergo σ- as well as π-dimer formation in solution.

The UV−vis spectrum of compound **5c** in toluene at room temperature displays (Figure 6A) an absorption maximum at 537 nm, a band that corresponds to the SOMO−LUMO transition, as confirmed by TD-DFT calculations (UB3LYP/6-31G(d,p)). As a result of the extended π-conjugation, the LUMO-α energy of **5c** (−1.41 eV) is lowered when compared

DOI: 10.1021/acs.joc.6b02246
J. Org. Chem. 2016, 81, 12303−12317

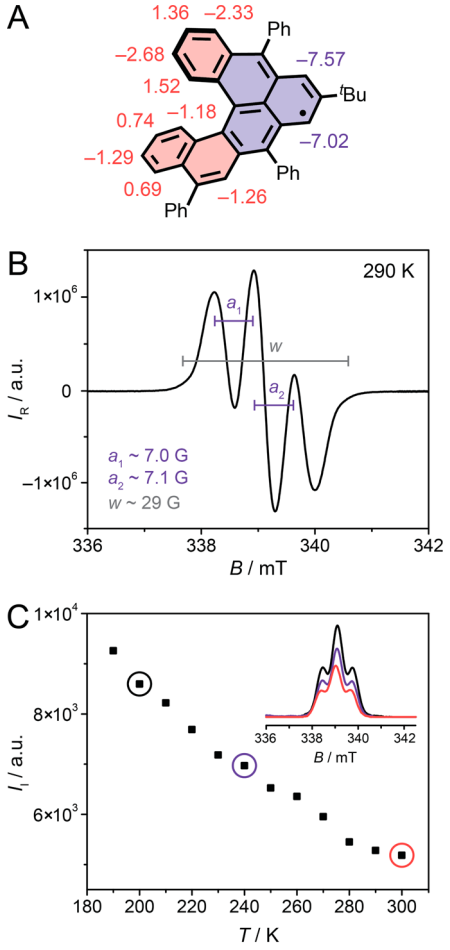

Figure 5. (A) Values of the proton hyperfine coupling constants (a_H) for **5c** obtained by DFT calculations (UB3LYP/EPR-III) on the optimized geometry (UB3LYP/6-31G(d,p)), (B) EPR spectrum of **5c** (toluene, 1.3×10^{-4} M) at 290 K, and (C) plot of intensity (I_I) values of the integrated EPR signals of **5c** (inset, 1.5×10^{-5} M) at different temperatures. I_R = relative intensity.

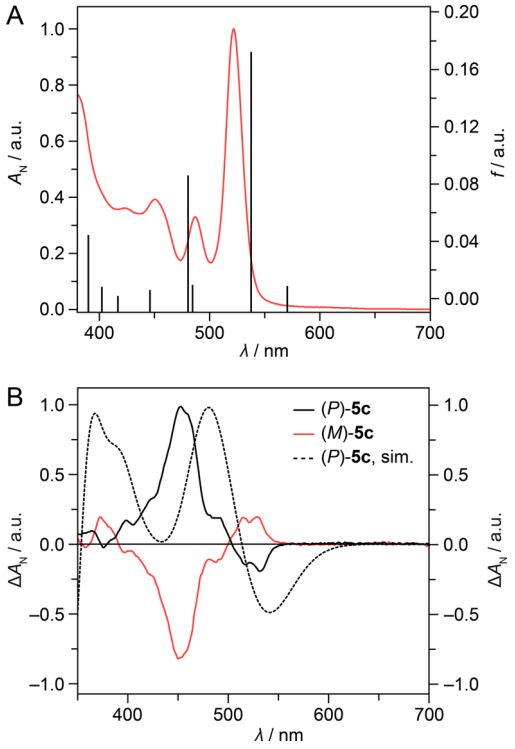

Figure 6. (A) Measured (toluene, 10^{-4} M, 25 °C; red line) and calculated (TD-DFT/UB3LYP/6-31G(d,p); black lines) UV−vis spectra and (B) measured (*tert*-butyl methyl ether, 25 °C; black solid line for (*P*)- and red solid line for (*M*)-enantiomer) and simulated CD spectra (TD-DFT/UB3LYP/6-31G(d,p); black dashed line for (*P*)-enantiomer) of **5c**. *f* = oscillator strength.

to that (−0.22 eV) of phenalenyl (DFT/UB3LYP/6-31G-(d,p)). Because the nonbonding SOMO-α have similar energies (−4.18 eV for **5c** and −4.32 eV for phenalenyl), the SOMO-α−LUMO-α energy gap of **5c** (2.77 eV) is significantly lowered compared to phenalenyl (4.18 eV). Consequently, the SOMO−LUMO transition of **5c** displays a bathochromic shift compared with phenalenyl.

To confirm the helical character of **5c**, the enantiomers of hydro-precursor **15** were separated by HPLC employing a chiral stationary phase and *n*-heptane/*tert*-butyl methyl ether (9:1) solvent mixture as the eluent (20 °C). The enantiomers displayed mirror-image CD spectra (Figure S21) and their enantiomeric purity was confirmed by resubjecting the separated fractions to HPLC (Figure S20). The absolute configuration of the enantiomers was determined with the aid of TD-DFT calculations (B3LYP/6-31G(d,p)), and the value of their racemization barrier, obtained by time-dependent CD measurements performed on (*P*)-**15** at 298 K, was determined to be (24.61 ± 0.03) kcal mol^{-1} (Figure S22), a value marginally higher than that (24.1 kcal mol^{-1} at 298 K[17]) of [5]helicene. The oxidation of (*P*)-**15** and (*M*)-**15** with an excess of CA afforded the two enantiomers of chiral neutral radical **5c**, (*P*)-**5c** and (*M*)-**5c**, respectively, which displayed complementary CD spectra that were in good agreement with spectra simulated by TD-DFT calculations (UB3LYP/6-31G(d,p); Figure 6B). Each of the enantiomers gave a three-broad-line EPR spectrum identical to that of racemic **5c**.

CONCLUSION

We have synthesized and studied two substituted derivatives of naphtho[3,2,1-*no*]tetraphene, the first example of a neutral open-shell hydrocarbon, which is helically chiral. In this spin-1/2 system, the spin density is delocalized over the entire nonplanar core composed of six rings, featuring a [5]helicene subunit. We have shown that the nonuniform spin-density distribution in this hydrocarbon promotes a highly selective σ-dimer formation as well as oxidation of the monosubstituted derivative. The dimerization process was fully suppressed in the case of the tetrasubstituted derivative, in which four substituents sterically hinder all of the reactive positions, and where both magnetic and chiroptical properties were integrated within a single molecule. Additionally, we have demonstrated that evaluation of aromaticity of the resonance structures that contribute to spin-delocalization can be used to qualitatively predict the distribution of spin density in conjugated open-shell molecules. This lesson of principles can be applied in rational design of helical systems, where spin-delocalization is extended beyond one turn of a helicene, for example, by incorporation of multiple phenalenyl units, and ultimately give rise to a new type of model systems for investigating phenomena arising from the interplay of chirality and magnetism.

DOI: 10.1021/acs.joc.6b02246
J. Org. Chem. 2016, 81, 12303−12317

EXPERIMENTAL SECTION

Materials and Instrumentation. All chemicals and solvents were purchased from commercial sources and were used without further purification unless stated otherwise. The reactions and experiments that are sensitive to oxygen were performed using Schlenk techniques and argon-saturated solvents. The solvents were saturated with argon by either passing argon gas through the solvent or using the freeze–pump–thaw technique in three cycles. The NMR experiments were performed on NMR spectrometers operating at 400, 500, 600, or 700 MHz proton frequencies. The instruments were equipped with a direct-observe 5 mm BBFO smart probe (400 and 600 MHz), an indirect-detection 5 mm BBI probe (500 MHz), a five-channel cryogenic 5 mm QCI probe (600 MHz), or a four-channel cryogenic 5 mm TCI probe (700 MHz). All probes were equipped with actively shielded *z*-gradients (10 A). The experiments were performed at 295 or 298 K unless indicated otherwise and the temperatures were calibrated using a methanol standard showing accuracy within ±0.2 K. Standard pulse sequences were used and the data was processed using 2-fold zero-filling in the indirect dimension for all 2D experiments. The highly deuterium-enriched benzene (C_6D_6, > 99.96% D) was used in NMR experiments. Chemical shifts (δ) are reported[18] in parts per million (ppm) relative to the solvent residual peak (^{1}H and ^{13}C NMR, respectively): C_6D_6 (δ = 7.16 and 128.06 ppm), $CDCl_3$ (δ = 7.26 and 77.16 ppm), CD_2Cl_2 (δ = 5.32 and 53.84 ppm), and CD_3OD (δ = 3.31 and 49.00 ppm). The UV–vis spectra were recorded in toluene at room temperature. The EPR spectra were recorded in an argon-saturated toluene (~10^{-4} M, unless stated otherwise) on an X-band CW-EPR spectrometer (9.66 GHz), equipped with a variable-temperature-control continuous-flow-N_2 cryostat. The *g*-factor corrections were obtained by using DPPH (g = 2.0037) as a standard. The HPLC separation of enantiomers of **15** was performed on an HPLC instrument equipped with a diode array UV–vis detector (λ = 200–600 nm) and a chiral-stationary-phase column (Chiralpak IE, 0.46 × 25 cm). Sample injection: 25 μL of a solution of **15** in heptane/*t*-BuMeO (1:1, ~ 1 mg in 1 mL). Separation: heptane/*t*-BuMeO (9:1), flow rate 1.0 mL min^{-1}, 293 K. The CD measurements were performed on a CD spectrometer in heptane/*t*-BuMeO (9:1, **15**) or *t*-BuMeO (**5c**) at 298 K in a 1 cm quartz glass cuvettes. All solutions were prepared and measured under argon-saturated conditions.

Synthesis. The synthesis of the parent compound **5a** was attempted starting from racemic 3-bromodibenzo[*c*,*g*]phenanthrene[13] (**18**, Scheme S1). The Friedel–Crafts acylation step did not, however, afford the desired intermediate **22a**. Instead, the planar byproducts **23** and **24** formed and were isolated. A similar result was obtained in an attempt to synthesize a monosubstituted derivative of **5a** starting from **18**. Instead of the expected product **22b**, the Friedel–Crafts acylation step yielded planar byproduct **29**. In both cases, the intramolecular acylation occurred mainly (**22a**) or exclusively (**22b**) at the 4- instead of the 2-position, and was accompanied by an intramolecular cyclization leading to planarization. Compound **6**, in which the 4-position is blocked by a phenyl substituent, was therefore used as the starting material in the synthesis of mono- and tetrasubstituted hydro-precursors **9a** and **9b** (Scheme S2). Compound **6** was synthesized from 3,4-dibromodibenzo[*c*,*g*]phenanthrene (**30**), which was prepared according to the previously described[13] procedure. All compounds were characterized by ^{1}H and ^{13}C NMR spectroscopy and MALDI-ToF mass spectrometry (MS). Compounds **7**, **8**, **9a**, **9b**, **10**, **15**, **23**, **24**, **29**, and **34** were additionally characterized by COSY/TOCSY, NOESY, HMQC, and HMBC NMR techniques and their structures were confirmed by assigning the ^{1}H and ^{13}C NMR resonances to the corresponding atoms. For the copies of the ^{1}H and ^{13}C NMR spectra, see Section S10. For the copies of MALDI-ToF MS and ESI-HRMS spectra, see Section S11. The solid-state structures of compounds **15** and **29** were confirmed (see Section S8) by X-ray diffraction (XRD) analysis of the corresponding single crystals. The separation of enantiomers of **15** by HPLC is described in Section S5.

*(±)-Methyl (E)-3-(dibenzo[c,g]phenanthren-3-yl)acrylate (**19**).* A mixture of **18** (147 mg, 0.406 mmol), methyl acrylate (145 mg, 1.64 mmol), PPh_3 (43 mg, 0.16 mmol), $Pd(OAc)_2$ (19 mg, 0.085 mmol), K_2CO_3 (114 mg, 0.825 mmol), tetrabutylammonium bromide (132 mg, 0.409 mmol), and DMF (10 mL) was heated at 100 °C for 20 h under an argon atmosphere before the reaction mixture was poured into water and extracted with CH_2Cl_2. The combined organic layers were washed with brine, dried over anhydrous Na_2SO_4, and filtered. After evaporation of the solvents, the residue was purified by column chromatography over silica gel using cyclohexane/CH_2Cl_2 (7:3) as an eluent to afford the desired product (128 mg, 86%) as a yellow solid. ^{1}H NMR (400 MHz, CD_2Cl_2, ppm) δ 8.62 (d, J = 15.8 Hz, 1H), 8.40 (dddd, J = 8.6, 1.4, 0.7, 0.7 Hz, 1H), 8.35 (dddd, J = 8.6, 1.4, 0.7, 0.7 Hz, 1H), 8.24 (d, J = 8.9 Hz, 1H), 8.16 (s, 1H), 8.04 (d, J = 8.6 Hz, 1H), 8.01–7.98 (m, 2H), 7.97 (d, J = 8.7 Hz, 1H), 7.91 (d, J = 8.6 Hz, 1H), 7.56 (ddd, J = 8.0, 6.6, 1.2 Hz, 1H), 7.54 (ddd, J = 8.0, 6.6, 1.2 Hz, 1H), 7.27 (ddd, J = 8.5, 6.9, 1.5 Hz, 1H), 7.26 (ddd, J = 8.6, 6.8, 1.4 Hz, 1H), 6.68 (d, J = 15.7 Hz, 1H), 3.86 (s, 3H). ^{13}C NMR (101 MHz, CD_2Cl_2, ppm) δ 167.4, 142.1, 133.4, 132.6, 131.9, 131.2, 131.1, 131.0, 130.3, 129.6, 129.3, 128.44, 128.40, 128.3, 128.2, 128.02, 127.96, 127.2, 127.1, 126.7, 126.5, 125.2, 125.1, 121.8, 121.7, 52.1. MALDI-ToF MS (m/z) calcd for $C_{26}H_{18}O_2$ 362.13, found 362.14 ($[M]^+$). ESI-HRMS (m/z) calcd for $C_{26}H_{18}O_2 + Na^+$ 385.1199, found 385.1200 (|Δ| = 0.2 ppm).

*(±)-Methyl 3-(dibenzo[c,g]phenanthren-3-yl)propanoate (**20**).* To a mixture of **19** (100 mg, 0.276 mmol) and CuCl (20 mg, 0.21 mmol) in CH_2Cl_2/EtOH (20 mL, 1:1), $NaBH_4$ (0.21 g, 5.5 mmol) was added in 10 portions at 0 °C over 2 h. The reaction mixture was quenched with aqueous HCl (2 M) and extracted with CH_2Cl_2. The combined organic layers were washed with saturated aqueous $NaHCO_3$, water, and brine, dried over anhydrous Na_2SO_4, and filtered. After evaporation of the solvents, the residue was purified by column chromatography over silica gel using cyclohexane/CH_2Cl_2 (7:3) as an eluent to afford the desired product (60 mg, 59%) as a pale yellow solid. ^{1}H NMR (400 MHz, CD_2Cl_2, ppm) δ 8.42 (dddd, J = 8.6, 1.3, 0.7, 0.7 Hz, 1H), 8.35 (dddd, J = 8.6, 1.3, 0.7, 0.7 Hz, 1H), 8.12 (d, J = 8.9 Hz, 1H), 8.00 (d, J = 8.5 Hz, 1H), 8.00–7.93 (m, 2H), 7.93 (d, J = 8.6 Hz, 1H), 7.85 (d, J = 8.5 Hz, 1H), 7.77 (s, 1H), 7.53 (ddd, J = 8.1, 6.8, 1.1 Hz, 1H), 7.50 (ddd, J = 8.1, 6.8, 1.1 Hz, 1H), 7.25 (ddd, J = 8.6, 6.9, 1.7 Hz, 1H), 7.25 (ddd, J = 8.6, 6.9, 1.7 Hz, 1H), 3.70 (s, 3H), 3.63–3.46 (m, 2H), 2.95–2.79 (m, 2H). ^{13}C NMR (101 MHz, CD_2Cl_2, ppm) δ 173.5, 135.9, 132.8, 132.4, 132.2, 131.4, 131.1, 131.0, 129.8, 129.2, 128.3, 128.03, 128.00, 127.9, 127.8, 127.5, 126.7, 126.38, 126.36, 126.2, 124.9, 124.8, 121.9, 52.0, 35.2, 28.6. MALDI-ToF MS (m/z) calcd for $C_{26}H_{20}O_2$ 364.15, found 364.12 ($[M]^+$). ESI-HRMS (m/z) calcd for $C_{26}H_{20}O_2 + H^+$ 365.1536, found 365.1535 (|Δ| = 0.4 ppm).

*(±)-3-(Dibenzo[c,g]phenanthren-3-yl)propanoic acid (**21**).* A mixture of **20** (60 mg, 0.16 mmol), lithium iodide (155 mg, 1.16 mmol), and 2,4,6-collidine (2.5 mL) was heated at 185 °C for 2 h under an argon atmosphere. The reaction mixture was cooled to room temperature and concentrated in a vacuum. To the residue, aqueous HCl (10 mL, 2 M) was added, and the precipitate that formed was filtered and washed with water to give the desired product (52 mg, 90%) as a brown solid, which was used in the next step without further purification. ^{1}H NMR (400 MHz, CD_2Cl_2, ppm) δ 8.40 (d, J = 8.6 Hz, 1H), 8.33 (d, J = 8.5 Hz, 1H), 8.12 (d, J = 8.9 Hz, 1H), 8.08–7.90 (m, 4H), 7.86 (d, J = 8.6 Hz, 1H), 7.79 (s, 1H), 7.61–7.45 (m, 2H), 7.34–7.16 (m, 2H), 3.68–3.45 (m, 2H), 3.03–2.80 (m, 2H). MALDI-ToF MS (m/z) calcd for $C_{25}H_{18}O_2$ 350.13, found 350.12 ($[M]^+$).

*(±)-4,5-Dihydro-6H-naphtho[3,2,1-no]tetraphen-6-one (**22a**).* A solution of **21** (50 mg, 0.13 mmol) in oxalyl chloride (5 mL) was heated at 65 °C for 3 h before the excess of oxalyl chloride was removed under the reduced pressure. The crude product was dissolved in CH_2Cl_2 (10 mL) and the solution was cooled to −78 °C. $AlCl_3$ (52 mg, 0.39 mmol) was added and the reaction mixture was allowed to warm to −10 °C over 5 h before it was poured onto ice and acidified with aqueous HCl (2 M). The organic layer was separated and the aqueous layer was extracted with CH_2Cl_2. The combined organic layers were washed with saturated aqueous $NaHCO_3$, water, and brine, dried over anhydrous Na_2SO_4, and filtered. After evaporation of the solvents, the residue was purified by column chromatography over silica gel using cyclohexane/CH_2Cl_2 (4:1) as an eluent to afford

DOI: 10.1021/acs.joc.6b02246
J. Org. Chem. 2016, 81, 12303–12317

byproducts **23** (8 mg, 18%) and **24** (16 mg, 37%) as yellow solids. The desired product **22a** was not observed.

*9,10-Dihydro-8H-naphtho[3,2,1,8-pqra]perylen-8-one (**23**).* ^{1}H NMR (500 MHz, CD_2Cl_2, ppm) δ 9.09 (dd, J = 7.8, 1.0 Hz, 1H), 9.00 (dd, J = 7.9, 1.0 Hz, 1H), 8.76 (d, J = 0.6 Hz, 1H), 8.37 (ddd, J = 7.8, 1.0, 0.6 Hz, 1H), 8.29 (t, J = 1.2 Hz, 1H), 8.23 (dd, J = 7.7, 1.0 Hz, 1H), 8.15−8.11 (m, 2H), 8.08 (dd, J = 7.8, 7.8 Hz, 1H), 8.04 (dd, J = 7.8, 7.8 Hz, 1H), 3.81−3.77 (m, 2H), 3.20−3.14 (m, 2H). ^{13}C NMR (From HMQC and HMBC, 500 MHz, CD_2Cl_2, ppm) δ 198.9, 132.4, 132.1, 131.5, 131.0, 130.1, 129.7, 129.6, 129.4, 128.5, 128.1, 127.6, 127.5 (2 ×), 127.2, 126.9, 126.8, 125.9, 125.1, 123.4, 122.9, 121.5, 39.5, 29.6 (one resonance could not be determined, see page S28). MALDI-ToF MS (m/z) calcd for $C_{25}H_{14}O$ 330.10, found 330.17 ($[M]^+$). ESI-HRMS (m/z) calcd for $C_{25}H_{14}O + H^+$ 331.1117, found 331.1115 (|Δ| = 0.8 ppm).

*2,3-Dihydro-1H-indeno[4,5,6,7-ghi]perylen-1-one (**24**).* ^{1}H NMR (500 MHz, CD_2Cl_2, ppm) δ 9.47 (d, J = 8.9 Hz, 1H), 9.05 (dd, J = 7.8, 1.0 Hz, 1H), 9.04 (dd, J = 7.9, 1.0 Hz, 1H), 8.26 (ddd, J = 7.7, 0.8, 0.8 Hz, 1H), 8.24 (dd, J = 8.9, 0.5 Hz, 1H), 8.24 (d, J = 8.9 Hz, 1H), 8.24−8.22 (m, 1H), 8.16 (dd, J = 8.8, 0.5 Hz, 1H), 8.10 (dd, J = 7.8, 7.8 Hz, 1H), 8.06 (dd, J = 7.7, 7.7 Hz, 1H), 3.73−3.69 (m, 2H), 3.05−3.01 (m, 2H). ^{13}C NMR (From HMQC and HMBC, 500 MHz, CD_2Cl_2, ppm) δ 208.4, 154.6, 133.9, 132.3, 131.6, 130.3, 130.0, 128.7, 128.4, 128.1, 127.8 (2 ×), 127.5, 126.9, 126.3, 126.2, 126.1, 125.6, 123.8, 123.2, 123.1, 121.9, 121.6, 37.5, 24.8. MALDI-ToF MS (m/z) calcd for $C_{25}H_{14}O$ 330.10, found 330.08 ($[M]^+$). ESI-HRMS (m/z) calcd for $C_{25}H_{14}O + H^+$ 331.1117, found 331.1120 (|Δ| = 0.8 ppm).

*(±)-Dibenzo[c,g]phenanthrene-3-carbaldehyde (**25**).* To a cooled (−78 °C) solution of **18** (1.00 g, 2.80 mmol) in THF (70 mL), *n*-BuLi (4.4 mL, 7.0 mmol, 1.6 M in hexane) was added dropwise and the mixture was stirred at −78 °C for 2 h before DMF (4.1 mL, 53 mmol) was added. The reaction mixture was stirred for an additional 2 h at −78 °C and then it was quenched with saturated aqueous NH_4Cl and extracted with CH_2Cl_2. The combined organic layers were washed with water and brine, and dried over anhydrous Na_2SO_4. After evaporation of the solvents, the residue was purified by column chromatography over silica gel using cyclohexane/ethyl acetate (95:5) as an eluent to afford the desired product (725 mg, 85%) as a yellow solid. ^{1}H NMR (400 MHz, CD_2Cl_2, ppm) δ 10.51 (s, 1H), 9.29 (d, J = 8.9 Hz, 1H), 8.38 (s, 1H), 8.36 (d, J = 8.6 Hz, 1H), 8.34 (d, J = 8.7 Hz, 1H), 8.09 (d, J = 9.0 Hz, 1H), 8.05−7.97 (m, 4H), 7.60 (ddd, J = 8.0, 6.9, 1.2 Hz, 1H), 7.56 (ddd, J = 8.0, 6.9, 1.1 Hz, 1H), 7.29 (ddd, J = 8.4, 6.9, 1.4 Hz, 1H), 7.26 (ddd, J = 8.4, 6.9, 1.4 Hz, 1H). ^{13}C NMR (101 MHz, CD_2Cl_2, ppm) δ 193.5, 138.8, 134.4, 132.7, 131.2, 131.0, 130.78, 130.76, 130.5, 129.9, 129.6, 129.5, 129.4, 128.8, 128.4, 128.21, 128.17, 128.0, 127.3, 126.5, 125.4, 125.1, 122.2. MALDI-ToF MS (m/z) calcd for $C_{23}H_{14}O$ 306.10, found 306.12 ($[M]^+$). MALDI-ToF HRMS (m/z) calcd for $C_{23}H_{14}O^+$ 306.1039, found 306.1038 (|Δ| = 0.8 ppm).

*(±)-Dibenzo[c,g]phenanthren-3-ylmethanol (**26**).* A solution of **25** (600 mg, 1.96 mmol) and $NaBH_4$ (11 mg, 0.29 mmol) in CH_2Cl_2/EtOH (150 mL, 2:1) was stirred at room temperature for 2 h before the reaction was quenched by the addition of aqueous HCl (2 M). The organic layer was separated and the aqueous layer was extracted with CH_2Cl_2. The combined organic layers were washed with saturated aqueous $NaHCO_3$, water, and brine, dried over anhydrous Na_2SO_4, and filtered. After evaporation of the solvents, the residue was purified by column chromatography over silica gel using cyclohexane/ethyl acetate (9:1) as an eluent to afford the desired product (578 mg, 96%) as a pale yellow solid. ^{1}H NMR (400 MHz, CD_2Cl_2, ppm) δ 8.41 (d, J = 8.6 Hz, 1H), 8.36 (d, J = 8.5 Hz, 1H), 8.17 (d, J = 8.9 Hz, 1H), 8.04−7.92 (m, 5H), 7.89 (d, J = 8.6 Hz, 1H), 7.53 (ddd, J = 7.9, 6.6, 1.2 Hz, 1H), 7.52 (ddd, J = 7.9, 6.6, 1.2 Hz, 1H), 7.25 (ddd, J = 8.4, 6.8, 1.5 Hz, 1H), 7.25 (ddd, J = 8.4, 6.8, 1.5 Hz, 1H), 5.31−5.20 (m, 2H), 2.06−1.98 (m, 1H). ^{13}C NMR (101 MHz, CD_2Cl_2, ppm) δ 135.8, 133.0, 132.5, 132.0, 131.2, 131.1, 130.6, 129.6, 129.3, 128.3, 128.1, 128.0, 127.94, 127.89, 127.0, 126.8, 126.7, 126.60, 126.56, 124.9, 124.8, 122.0, 63.9. MALDI-ToF MS (m/z) calcd for $C_{23}H_{16}O$ 308.12, found 308.19 ($[M]^+$). MALDI-ToF HRMS (m/z) calcd for $C_{23}H_{16}O^+$ 308.1196, found 308.1195 (|Δ| = 0.1 ppm).

*(±)-3-(Bromomethyl)dibenzo[c,g]phenanthrene (**27**).* To a solution of **26** (550 mg, 1.78 mmol) in benzene (50 mL), PBr_3 (0.25 mL, 2.7 mmol) was added slowly and the resulting solution was heated at 95 °C for 1 h. The reaction mixture was cooled to room temperature, quenched with $NaHCO_3$, and extracted with CH_2Cl_2. The combined organic layers were washed with water and brine, dried over anhydrous Na_2SO_4, and filtered. After evaporation of the solvents, the residue was purified by column chromatography over silica gel using cyclohexane/CH_2Cl_2 (1:1) as an eluent to afford the desired product (565 mg, 86%) as a pale yellow solid. ^{1}H NMR (400 MHz, CD_2Cl_2, ppm) δ 8.39 (ddd, J = 8.6, 0.9, 0.9 Hz, 1H), 8.35 (ddd, J = 8.5, 1.0, 1.0 Hz, 1H), 8.23 (d, J = 8.8 Hz, 1H), 8.08 (d, J = 8.8 Hz, 1H), 8.01 (dd, J = 8.1, 1.4 Hz, 1H), 7.99−7.94 (m, 3H), 7.87 (d, J = 8.6 Hz, 1H), 7.55 (ddd, J = 8.0, 6.8, 1.1 Hz, 1H), 7.53 (ddd, J = 8.0, 6.8, 1.1 Hz, 1H), 7.26 (ddd, J = 8.3, 7.0, 1.2 Hz, 1H), 7.26 (ddd, J = 8.3, 7.0, 1.2 Hz, 1H), 5.17 (d, J = 10.5 Hz, 1H), 5.09 (d, J = 10.4 Hz, 1H). ^{13}C NMR (101 MHz, CD_2Cl_2, ppm) δ 133.3, 132.7, 132.5, 131.8, 131.2, 131.0, 130.1, 129.6, 129.4, 129.2, 128.5, 128.4, 128.3, 128.09, 128.05, 128.0, 127.1, 127.0, 126.3, 125.1, 125.0, 121.9, 32.6. MALDI-ToF MS (m/z) calcd for $C_{23}H_{15}Br$ 370.04, found 369.00 ($[M - H]^+$).

*(±)-2-(Dibenzo[c,g]phenanthren-3-ylmethyl)-3,3-dimethylbutanoic acid (**28**).* To a cooled (−78 °C) solution of methyl *tert*-butylacetate (0.53 mL, 3.5 mmol) in THF (15 mL), LDA (1.73 mL, 3.47 mmol, 2 M in THF/heptane) was added dropwise and the mixture was stirred at −78 °C for 2 h. While maintaining the temperature, a suspension of **27** (322 mg, 0.867 mmol) in THF (10 mL) was then added and the reaction mixture was allowed to warm to room temperature overnight before it was quenched with saturated aqueous NH_4Cl and extracted with CH_2Cl_2. The combined organic layers were washed with water and brine, and dried over anhydrous Na_2SO_4. After filtration and evaporation of the solvents, the residue was purified by column chromatography over silica gel using cyclohexane/CH_2Cl_2 (7:3) as an eluent to afford the methyl ester intermediate (247 mg, 68%) as a yellow solid. A mixture of this intermediate (220 mg, 0.523 mmol), lithium iodide (350 mg, 2.62 mmol), and 2,4,6-collidine (5 mL) was heated at 185 °C for 1 h under an argon atmosphere before it was cooled to room temperature and concentrated in a vacuum. To the residue, aqueous HCl (10 mL, 2 M) was added, and the precipitate that formed was filtered and washed with water to give the desired product (200 mg, 94%; 64% over two steps) as a brown solid and as an approximately 1:1 mixture of two possible diastereomers, which was used in the next step without further purification. ^{1}H NMR (400 MHz, CD_2Cl_2, ppm) δ 8.38 (d, J = 8.6 Hz, 2H), 8.31 (d, J = 8.6 Hz, 2H), 8.10 (d, J = 8.9 Hz, 1H), 8.05 (d, J = 8.8 Hz, 1H), 8.02−7.95 (m, 4H), 7.92 (d, J = 8.0 Hz, 2H), 7.86 (d, J = 8.6 Hz, 1H), 7.86 (d, J = 8.6 Hz, 1H), 7.77 (d, J = 8.5 Hz, 2H), 7.74 (d, J = 6.5 Hz, 2H), 7.55−7.45 (m, 4H), 7.27−7.18 (m, 4H), 3.60 (dd, J = 13.8, 2.6 Hz, 1H), 3.53 (dd, J = 14.0, 2.8 Hz, 1H), 3.41 (dd, J = 13.9, 12.4 Hz, 1H), 3.34 (dd, J = 13.8, 12.1 Hz, 1H), 2.83 (dd, J = 12.2, 2.6 Hz, 1H), 2.77 (dd, J = 11.9, 2.8 Hz, 1H), 1.22 (s, 9H), 1.20 (s, 9H). MALDI-ToF MS (m/z) calcd for $C_{29}H_{26}O_2$ 406.19, found 406.22 ($[M]^+$).

*(±)-5-(tert-Butyl)-4,5-dihydro-6H-naphtho[3,2,1-no]tetraphen-6-one (**22b**).* A solution of **28** (190 mg, 0.467 mmol) in oxalyl chloride (8 mL) was heated at 65 °C for 2 h before the excess of oxalyl chloride was removed under the reduced pressure. The crude acyl chloride intermediate was dissolved in CH_2Cl_2 (30 mL) and the solution was cooled to −78 °C. $AlCl_3$ (207 mg, 1.55 mmol) was added and the reaction mixture was allowed to warm to −10 °C over 5 h before it was poured onto ice and acidified with aqueous HCl (2 M). The organic layer was separated and the aqueous layer was extracted with CH_2Cl_2. The combined organic layers were washed with saturated aqueous $NaHCO_3$, water, and brine, dried over anhydrous Na_2SO_4, and filtered. After evaporation of the solvents, the residue was purified by column chromatography over silica gel using cyclohexane/CH_2Cl_2 (7:3) as an eluent to afford byproduct **29** (91 mg, 47%) as a yellow solid. The desired product **22b** was not observed.

*(±)-2-(tert-Butyl)-2,3-dihydro-1H-indeno[4,5,6,7-ghi]perylen-1-one (**29**).* ^{1}H NMR (500 MHz, CD_2Cl_2, ppm) δ 9.45 (d, J = 8.9 Hz, 1H), 8.97 (d, J = 7.8 Hz, 1H), 8.96 (d, J = 7.8 Hz, 1H), 8.23−8.20 (m,

DOI: 10.1021/acs.joc.6b02246
J. Org. Chem. 2016, 81, 12303−12317

2H), 8.19−8.16 (m, 2H), 8.11 (d, J = 8.9 Hz, 1H), 8.04 (dd, J = 7.6, 7.6 Hz, 1H), 8.01 (dd, J = 7.7, 7.5 Hz, 1H), 3.73 (dd, J = 17.3, 7.6 Hz, 1H), 3.53 (dd, J = 17.3, 3.9 Hz, 1H), 2.80 (dd, J = 7.8, 3.8 Hz, 1H), 1.19 (s, 9H). ^{13}C NMR (From HMQC and HMBC, 500 MHz, CD_2Cl_2, ppm) δ 209.7, 152.7, 133.9, 132.4, 131.7, 130.4, 130.0, 129.5, 128.5, 128.0, 127.9, 127.8, 127.5, 127.0, 126.5, 126.2, 126.0, 125.7, 124.0, 123.4 (2 ×), 122.0, 121.7, 57.8, 34.6, 29.0, 28.1. MALDI-ToF MS (m/z) calcd for $C_{29}H_{22}O$ 386.17, found 386.20 ($[M]^+$). MALDI-ToF HRMS (m/z) calcd for $C_{29}H_{22}O^+$ 386.1665, found 386.1665 (|Δ| = 0.1 ppm).

*(±)-3-Bromo-4-phenyldibenzo[c,g]phenanthrene (**6**).* A mixture of **30** (1.50 g, 3.44 mmol), phenylboronic acid (0.51 g, 4.1 mmol), K_2CO_3 (3.33 g, 24.1 mmol), $Pd(PPh_3)_4$ (0.12 g, 0.10 mmol), and toluene/EtOH/water (210 mL, 4:2:1) was heated at 90 °C for 30 min under an argon atmosphere before aqueous HCl (25 mL, 2 M) was added to quench the reaction. The reaction mixture was then extracted with CH_2Cl_2 (3 × 25 mL) and the combined organic layers were washed with brine, dried over anhydrous Na_2SO_4, and filtered. After evaporation of the solvents, the residue was purified by column chromatography over silica gel using cyclohexane as an eluent to afford the desired product (602 mg, 40%) as a white solid. ^{1}H NMR (400 MHz, $CDCl_3$, ppm) δ 8.54 (d, J = 8.9 Hz, 1H), 8.39 (dddd, J = 8.6, 1.4, 0.7, 0.7 Hz, 1H), 8.37 (dddd, J = 8.6, 1.4, 0.7, 0.7 Hz, 1H), 8.04 (d, J = 8.9 Hz, 1H), 8.00 (dd, J = 8.1, 1.3 Hz, 1H), 7.91 (dd, J = 8.1, 1.3 Hz, 1H), 7.77 (d, J = 8.8 Hz, 1H), 7.62−7.50 (m, 5H), 7.46 (d, J = 8.9 Hz, 1H), 7.42−7.36 (m, 2H), 7.28 (ddd, J = 8.4, 7.0, 1.4 Hz, 1H), 7.27 (ddd, J = 8.4, 7.0, 1.4 Hz, 1H). ^{13}C NMR (101 MHz, $CDCl_3$, ppm) δ 140.9, 139.9, 132.5, 132.1, 132.0, 131.0, 130.7, 130.5, 130.4, 129.8, 129.7 (two overlapped signals), 128.69, 128.67, 128.5, 128.3, 127.9, 127.82 (two overlapped signals), 127.80, 127.0, 126.8, 126.6, 125.8, 125.1, 125.0, 124.7, 124.0. MALDI-ToF MS (m/z) calcd for $C_{28}H_{17}Br$ 432.05, found 431.71 ($[M]^+$). MALDI-ToF HRMS (m/z) calcd for $C_{28}H_{17}Br^+$ 432.0508, found 432.0508 (|Δ| = 0.1 ppm).

*(±)-Methyl (E)-3-(4-phenyldibenzo[c,g]phenanthren-3-yl)-acrylate (**7**).* A mixture of **6** (450 mg, 1.04 mmol), methyl acrylate (358 mg, 4.16 mmol), PPh_3 (0.11 g, 0.42 mmol), $Pd(OAc)_2$ (47 mg, 0.21 mmol), K_2CO_3 (287 mg, 2.08 mmol), tetrabutylammonium bromide (335 mg, 1.04 mmol), and DMF (20 mL) was heated at 100 °C for 20 h under an argon atmosphere before the reaction mixture was poured into water and extracted with CH_2Cl_2. The combined organic layers were washed with brine, dried over anhydrous Na_2SO_4, and filtered. After evaporation of the solvents, the residue was purified by column chromatography over silica gel using cyclohexane/ethyl acetate (99:1) as an eluent to afford the desired product (400 mg, 88%) as a pale yellow solid. ^{1}H NMR (500 MHz, CD_2Cl_2, ppm) δ 8.34 (dddd, J = 8.6, 1.4, 0.7, 0.7 Hz, 1H), 8.34 (dddd, J = 8.6, 1.4, 0.7, 0.7 Hz, 1H), 8.23 (d, J = 8.9 Hz, 1H), 8.00 (ddd, J = 8.9, 0.6, 0.6 Hz, 1H), 7.99 (dddd, J = 8.0, 1.3, 0.6, 0.6 Hz, 1H), 7.93 (dddd, J = 7.9, 1.3, 0.6, 0.6 Hz, 1H), 7.92 (d, J = 16.4 Hz, 1H), 7.81 (ddd, J = 8.9, 0.7, 0.7 Hz, 1H), 7.58−7.48 (m, 6H), 7.37−7.31 (m, 2H), 7.26 (ddd, J = 8.5, 6.9, 1.2 Hz, 1H), 7.26 (ddd, J = 8.5, 6.9, 1.2 Hz, 1H), 6.05 (d, J = 16.4 Hz, 1H), 3.73 (s, 3H). ^{13}C NMR (101 MHz, CD_2Cl_2, ppm) δ 166.9, 143.5, 139.0, 138.7, 132.7, 132.5, 131.9, 131.3, 131.1, 131.0, 130.9, 130.6, 129.8 (two overlapped signals), 129.7, 128.9, 128.7, 128.2, 128.1 (two overlapped signals), 128.0, 127.7 (two overlapped signals), 127.3, 127.1, 127.0, 126.2, 125.2 (two overlapped signals), 124.8, 123.5, 51.9. MALDI-ToF MS (m/z) calcd for $C_{32}H_{22}O_2$ 438.16, found 438.59 ($[M]^+$). MALDI-ToF HRMS (m/z) calcd for $C_{32}H_{22}O_2^+$ 438.1614, found 438.1614 (|Δ| = 0.2 ppm).

*(±)-Methyl 3-(4-phenyldibenzo[c,g]phenanthren-3-yl)-propanoate (**31**).* Compound 7 (0.35 g, 0.80 mmol) and Pd/C (84 mg, 5% palladium on charcoal) were suspended in CH_2Cl_2/EtOH (20 mL, 1:1), and hydrogen gas was passed through the suspension for 30 min. The reaction mixture was then stirred at room temperature under a hydrogen atmosphere for 24 h before it was passed through Celite to afford, after evaporation of the solvents, the desired product (345 mg, 98%) as a pale yellow oil, which was used in the next step without further purification. ^{1}H NMR (400 MHz, CD_2Cl_2, ppm) δ 8.34 (dddd, J = 8.5, 1.3, 0.7, 0.7 Hz, 1H), 8.31 (dddd, J = 8.6, 1.3, 0.7, 0.7 Hz, 1H), 8.17 (d, J = 8.9 Hz, 1H), 8.04 (d, J = 8.8 Hz, 1H), 7.99 (dd, J = 8.1, 1.4 Hz, 1H), 7.91 (dd, J = 8.0, 1.4 Hz, 1H), 7.76 (d, J = 8.7 Hz, 1H), 7.61−7.51 (m, 4H), 7.49 (ddd, J = 8.0, 6.8, 1.1 Hz, 1H), 7.38−7.31 (m, 3H), 7.25 (ddd, J = 8.4, 6.8, 1.4 Hz, 1H), 7.24 (ddd, J = 8.4, 6.8, 1.4 Hz, 1H), 3.63 (s, 3H), 3.32 (ddd, J = 14.0, 10.8, 6.3 Hz, 1H), 3.25 (ddd, J = 14.0, 10.7, 6.5 Hz, 1H), 2.62 (ddd, J = 16.9, 10.6, 6.3 Hz, 1H), 2.56 (ddd, J = 16.5, 10.8, 6.5 Hz, 1H). ^{13}C NMR (101 MHz, CD_2Cl_2, ppm) δ 173.2, 140.1, 138.8, 133.7, 132.3, 132.2, 131.8, 131.4, 131.1, 130.9, 130.4, 130.1, 129.8, 129.7, 129.1, 128.9, 128.2, 128.0, 127.92, 127.88, 127.5, 127.3, 126.7, 126.6, 126.3, 125.01, 124.99, 124.98, 122.3, 51.9, 35.4, 26.0. MALDI-ToF MS (m/z) calcd for $C_{32}H_{24}O_2$ 440.18, found 440.62 ($[M]^+$). MALDI-ToF HRMS (m/z) calcd for $C_{32}H_{24}O_2^+$ 440.1771, found 440.1770 (|Δ| = 0.2 ppm).

*(±)-3-(4-Phenyldibenzo[c,g]phenanthren-3-yl)propanoic acid (**32**).* A mixture of **31** (340 mg, 0.772 mmol), lithium iodide (0.72 g, 5.4 mmol), and 2,4,6-collidine (10 mL) was heated at 185 °C for 1 h under an argon atmosphere before the reaction mixture was cooled to room temperature and concentrated in a vacuum. To the residue, aqueous HCl (15 mL, 2 M) was added, and the precipitate that formed was filtered and washed with water to afford the desired product (293 mg, 89%) as a brown solid, which was used in the next step without further purification. ^{1}H NMR (400 MHz, CD_3OD, ppm) δ 8.23 (d, J = 8.7 Hz, 1H), 8.20 (d, J = 8.6 Hz, 1H), 8.18 (d, J = 9.0 Hz, 1H), 8.04 (d, J = 8.9 Hz, 1H), 7.98 (d, J = 8.0 Hz, 1H), 7.88 (d, J = 8.0 Hz, 1H), 7.73 (d, J = 8.9 Hz, 1H), 7.60−7.43 (m, 4H), 7.36−7.25 (m, 4H), 7.23−7.15 (m, 2H), 3.34−3.16 (m, 2H), 2.64−2.47 (m, 2H). MALDI-ToF MS (m/z) calcd for $C_{31}H_{22}O_2$ 426.16, found 426.14 ($[M]^+$).

*(±)-3-Phenyl-4,5-dihydro-6H-naphtho[3,2,1-no]tetraphen-6-one (**8**).* A solution of **32** (220 mg, 0.516 mmol) in oxalyl chloride (11 mL) was heated at 65 °C for 3 h before the excess of oxalyl chloride was removed under the reduced pressure. The crude acid chloride intermediate was dissolved in CH_2Cl_2 (50 mL) and the solution was cooled to −78 °C. Solid $AlCl_3$ (191 mg, 1.42 mmol) was added and the reaction mixture was allowed to warm to −10 °C over 5 h before it was poured onto ice and acidified with aqueous HCl (2 M). The organic layer was separated and the aqueous layer was extracted with CH_2Cl_2. The combined organic layers were washed with saturated aqueous $NaHCO_3$, water, and brine, dried over anhydrous Na_2SO_4, and filtered. After evaporation of the solvents, the residue was purified by column chromatography over silica gel using cyclohexane/CH_2Cl_2 (7:3) as an eluent to afford the desired product (120 mg, 62%) as a pale yellow solid. ^{1}H NMR (500 MHz, CD_2Cl_2, ppm) δ 8.77 (dd, J = 0.7, 0.7 Hz, 1H), 8.39 (dddd, J = 8.6, 1.4, 0.7, 0.7 Hz, 1H), 8.33 (dddd, J = 8.5, 1.4, 0.7, 0.7 Hz, 1H), 8.16 (dddd, J = 8.1, 1.3, 0.6, 0.6 Hz, 1H), 7.94 (dddd, J = 8.0, 1.3, 0.6, 0.6 Hz, 1H), 7.83 (ddd, J = 8.7, 0.7, 0.5 Hz, 1H), 7.63−7.51 (m, 5H), 7.51 (d, J = 8.9 Hz, 1H), 7.42 (dddd, J = 7.4, 2.0, 1.4, 0.7 Hz, 1H), 7.37 (ddd, J = 8.4, 6.9, 1.4 Hz, 1H), 7.32 (dddd, J = 7.3, 1.7, 1.7, 0.7 Hz, 1H), 7.27 (ddd, J = 8.4, 6.9, 1.4 Hz, 1H), 3.22−3.10 (m, 2H), 2.96−2.83 (m, 2H). ^{13}C NMR (101 MHz, CD_2Cl_2, ppm) δ 198.4, 139.3, 137.7, 133.7, 132.3, 131.8, 131.3, 131.2, 130.9, 130.7, 130.4, 130.2, 129.7, 129.51, 129.50, 129.2, 129.0, 128.3, 128.1, 128.02, 127.98, 127.9, 127.5, 127.24, 127.15, 126.8, 125.8, 125.2, 124.7, 38.7, 26.9. MALDI-ToF MS (m/z) calcd for $C_{31}H_{20}O$ 408.15, found 408.66 ($[M]^+$). MALDI-ToF HRMS (m/z) calcd for $C_{31}H_{20}O^+$ 408.1509, found 408.1509 (|Δ| = 0.0 ppm).

*(±)-3-Phenyl-5,6-dihydro-4H-naphtho[3,2,1-no]tetraphen-6-ol (**33**).* A solution of **8** (60 mg, 0.15 mmol) and $NaBH_4$ (11 mg, 0.29 mmol) in CH_2Cl_2/EtOH (30 mL, 2:1) was stirred at room temperature for 2 h before the reaction was quenched by the addition of aqueous HCl (2 M). The organic layer was separated and the aqueous layer was extracted with CH_2Cl_2. The combined organic layers were washed with saturated aqueous $NaHCO_3$, water, and brine, dried over anhydrous Na_2SO_4, and filtered. After evaporation of the solvents, the residue was purified by column chromatography over silica gel using cyclohexane/CH_2Cl_2 (1:1) as an eluent to give the desired product (54 mg, 90%) as a yellow solid and as an approximately 1:1 mixture of two possible diastereomers. ^{1}H NMR (400 MHz, CD_2Cl_2, ppm) δ 8.35−8.29 (m, 4H), 8.09 (dd, J = 1.0, 1.0 Hz, 1H), 8.09 (dd, J = 1.0, 1.0 Hz, 1H), 7.99 (dd, J = 8.1, 1.4 Hz, 1H), 7.98 (dd, J = 8.1, 1.4 Hz, 1H), 7.91 (dd, J = 7.9, 1.4 Hz, 1H), 7.91 (dd, J = 7.9, 1.4 Hz, 1H), 7.77 (d, J = 8.8 Hz, 1H), 7.77 (d, J = 8.8 Hz, 1H),

DOI: 10.1021/acs.joc.6b02246
J. Org. Chem. 2016, 81, 12303−12317

7.61−7.42 (m, 12H), 7.38−7.31 (m, 4H), 7.26−7.19 (m, 4H), 5.28 (ddd, J = 7.9, 4.4, 4.4 Hz, 1H), 5.18 (ddd, J = 7.7, 3.9, 3.9 Hz, 1H), 3.10 (ddd, J = 17.1, 8.5, 4.6 Hz, 1H), 3.06 (ddd, J = 17.1, 8.5, 4.6 Hz, 1H), 2.86 (ddd, J = 16.8, 7.7, 4.7 Hz, 1H), 2.85 (ddd, J = 16.8, 7.7, 4.7 Hz, 1H), 2.28−2.00 (m, 6H). ^{13}C NMR (101 MHz, CD_2Cl_2, ppm) δ (out of 62 signals expected for two possible diastereomers, seven signals could not be detected within the resolution limits of the NMR technique because of the signal overlap) 134.0, 137.1, 137.0, 136.2, 136.1, 132.22, 132.17, 132.07, 132.06, 132.02, 131.98, 131.5, 131.4, 131.3, 131.2, 131.11, 131.05, 130.4, 130.2, 129.69, 129.65, 129.62, 129.61, 129.13, 129.10, 128.9, 128.5, 128.13, 128.08, 128.07, 127.98, 127.97, 127.7, 127.4, 127.13, 127.08, 126.78, 126.77, 126.4, 126.0, 125.9, 125.7, 125.1, 124.94, 124.93, 124.85, 124.8, 124.70, 124.68, 70.1, 70.0, 31.8, 31.7, 25.8, 25.7. MALDI-ToF MS (m/z) calcd for $C_{31}H_{22}O$ 410.17, found 410.27 ($[M]^+$). MALDI-ToF HRMS (m/z) calcd for $C_{31}H_{22}O^+$ 410.1665, found 410.1665 (|Δ| = 0.1 ppm).

*(±)-3-Phenyl-4H-naphtho[3,2,1-no]tetraphene (**9a**).* *p*-Toluenesulfonic acid monohydrate (9 mg, 0.05 mmol) was added to a hot (80 °C) solution of **33** (40 mg, 0.097 mmol) in benzene (35 mL) and the reaction mixture was heated at 80 °C for 5−10 min before it was cooled in an ice bath and passed through a pad of silica gel using cyclohexane/CH_2Cl_2 (1:1) as an eluent to afford the desired product (27 mg, 71%) as a yellow solid. ^{1}H NMR (500 MHz, C_6D_6, ppm) δ 8.62 (dddd, J = 8.5, 1.2, 0.6, 0.6 Hz, 1H), 8.48 (dddd, J = 8.5, 1.3, 0.7, 0.7 Hz, 1H), 7.68 (dddd, J = 8.0, 1.3, 0.6, 0.6 Hz, 1H), 7.65 (dd, J = 7.9, 1.5 Hz, 1H), 7.55 (ddd, J = 8.8, 0.5, 0.5 Hz, 1H), 7.53 (d, J = 8.9 Hz, 1H), 7.36 (dddddd, J = 1.3, 1.3, 0.6, 0.6, 0.6, 0.6 Hz, 1H), 7.31 (dddd, J = 7.4, 7.4, 1.6, 0.7 Hz, 1H), 7.30 (dddd, J = 7.7, 7.4, 1.6, 0.7 Hz, 1H), 7.28−7.22 (m, 3H), 7.08 (m, J = 7.5 Hz, 1H), 7.02 (ddd, J = 8.4, 6.9, 1.4 Hz, 1H), 6.98 (m, J = 7.4 Hz, 1H), 6.95 (ddd, J = 8.4, 7.0, 1.5 Hz, 1H), 6.67 (dddd, J = 9.7, 2.2, 2.2, 0.5 Hz, 1H), 5.76 (dddd, J = 9.7, 4.3, 3.8, 0.5 Hz, 1H), 3.57 (dddd, J = 25.5, 3.8, 2.2, 1.3 Hz, 1H), 3.46 (dddd, J = 25.6, 4.4, 2.0, 1.1 Hz, 1H). ^{13}C NMR (101 MHz, C_6D_6, ppm) δ 140.2, 137.4, 133.3, 132.4, 131.9, 131.6, 131.5, 130.7, 130.6, 130.3, 130.2, 129.60, 129.59, 129.4, 128.6, 128.4, 128.0, 127.9, 127.70, 127.67, 127.6, 127.5 (two overlapped signals), 126.9, 126.5, 126.4, 124.9, 124.54, 124.53, 124.4, 32.5. MALDI-ToF MS (m/z) calcd for $C_{31}H_{20}$ 392.16, found 392.66 ($[M]^+$). MALDI-ToF HRMS (m/z) calcd for $C_{31}H_{20}^+$ 392.1560, found 392.1560 (|Δ| = 0.1 ppm).

*(±)-3-Phenyl-7H-naphtho[3,2,1-no]tetraphene (**9b**).* A mixture of **9a** (10 mg, 0.025 mmol) and TFA (1 drop) in CH_2Cl_2 (10 mL) was stirred for 10 min at room temperature before it was filtered through a short plug of silica gel using cyclohexane/CH_2Cl_2 (1:1) as an eluent to afford the desired product (8.5 mg, 85%) as a yellow solid. ^{1}H NMR (500 MHz, C_6D_6, ppm) δ 8.90 (d, J = 8.3 Hz, 1H), 7.81 (dd, J = 8.0, 1.1 Hz, 1H), 7.65−7.60 (m, 1H), 7.63 (d, J = 9.3 Hz, 1H), 7.51 (dd, J = 7.9, 1.4 Hz, 1H), 7.40 (dddd, J = 7.4, 1.5, 1.5, 0.8 Hz, 1H), 7.36−7.25 (m, 5H), 7.22 (ddd, J = 8.0, 7.1, 1.2 Hz, 1H), 7.19−7.13 (m, 3H), 7.03 (ddd, J = 8.4, 7.0, 1.4 Hz, 1H), 7.00 (ddd, J = 7.4, 7.4, 1.2 Hz, 1H), 6.78 (dddd, J = 8.3, 7.3, 1.2, 1.2 Hz, 1H), 4.38 (d, J = 18.0 Hz, 1H), 3.92 (d, J = 18.1 Hz, 1H). ^{13}C NMR (101 MHz, C_6D_6, ppm) δ 139.8, 137.5, 137.1, 135.9, 133.7, 133.1, 131.9, 131.8, 131.5, 131.3, 131.2, 130.90, 130.85, 130.8, 130.4, 128.9, 128.6, 128.5, 128.1, 127.7, 127.43, 127.38, 127.3, 126.6, 126.2, 126.0, 125.7, 125.1, 125.0, 124.0, 37.2. MALDI-ToF MS (m/z) calcd for $C_{31}H_{20}$ 392.16, found 392.21 ($[M]^+$). MALDI-ToF HRMS (m/z) calcd for $C_{31}H_{20}^+$ 392.1560, found 392.1560 (|Δ| = 0.1 ppm).

*(±)-3-Phenyl-3,7-dihydro-3,11b-epidioxynaphtho[3,2,1-no]tetraphene (**10**).* In the presence of oxygen and light, compound **9b** undergoes a clean transformation to **10** in solution. ^{1}H NMR (400 MHz, C_6D_6, ppm) δ 7.85 (dd, J = 7.9, 1.4 Hz, 1H), 7.80−7.76 (m, 2H), 7.51 (dddd, J = 8.2, 1.3, 0.6, 0.6 Hz, 1H), 7.42 (d, J = 8.5 Hz, 1H), 7.37 (d, J = 8.5 Hz, 1H), 7.35−7.29 (m, 2H), 7.28−7.23 (m, 1H), 7.22 (ddd, J = 7.8, 7.7, 1.4 Hz, 1H), 7.14 (dd, J = 8.8, 1.0 Hz, 1H), 7.12−7.09 (m, 2H), 7.05 (ddd, J = 8.1, 6.8, 1.1 Hz, 1H), 7.04 (dd, J = 7.7, 7.7 Hz, 1H), 6.90 (ddd, J = 8.8, 6.8, 1.4 Hz, 1H), 6.92 (dd, J = 7.6, 7.6 Hz, 1H), 6.84 (dddd, J = 7.7, 0.9, 0.9, 0.9 Hz, 1H), 3.86 (d, J = 21.0 Hz, 1H), 3.65 (d, J = 21.1 Hz, 1H). ^{13}C NMR (101 MHz, C_6D_6, ppm) δ 141.9, 141.0, 140.1, 136.6, 135.7, 134.6, 134.0, 131.9, 130.8, 130.4, 129.8, 129.4, 129.2, 129.0, 128.6, 128.4 (three overlapped signals), 127.2, 127.1, 126.6, 125.9, 125.54, 125.49, 122.3, 121.9, 84.1, 80.2, 32.03. ESI-HRMS (m/z) calcd for $C_{31}H_{20}O_2$ + H^+ 425.1542, found 425.1536 (|Δ| = 1.4 ppm). In the IR spectrum of **10**, no bands corresponding to the O−H stretches were visible, excluding the possibility of a dihydroxy product.

*(±)-3-Methyl-4-phenyldibenzo[c,g]phenanthrene (**11**).* A solution of methylmagnesium bromide (11.5 mL, 34.6 mmol, 3 M in Et_2O) was added dropwise to a cooled (0 °C) solution of **6** (2.50 g, 5.77 mmol) and $NiCl_2$(dppp) (0.22 g, 0.40 mmol) in dry Et_2O (300 mL) under an argon atmosphere. The reaction mixture was then allowed to warm to room temperature over 20 min before it was heated at reflux overnight. After cooling the reaction mixture to 0 °C, aqueous HCl (200 mL, 2 M) was added slowly to quench the reaction. The organic layer was separated and the aqueous layer was washed with Et_2O (3 × 50 mL). The combined organic layers were washed with brine, dried over anhydrous Na_2SO_4, and filtered. After evaporation of the solvents, the residue was purified by column chromatography over silica gel using cyclohexane as an eluent to afford the desired product (2.08 g, 98%) as a white solid. ^{1}H NMR (400 MHz, CD_2Cl_2, ppm) δ 8.36 (dddd, J = 8.5, 1.4, 0.6, 0.6 Hz, 1H), 8.32 (dddd, J = 8.5, 1.4, 0.6, 0.6 Hz, 1H), 8.20 (d, J = 8.9 Hz, 1H), 8.03 (ddd, J = 8.9, 0.7, 0.7 Hz, 1H), 7.99 (dddd, J = 8.0, 1.3, 0.6, 0.6 Hz, 1H), 7.91 (dddd, J = 8.0, 1.3, 0.6, 0.6 Hz, 1H), 7.76 (ddd, J = 8.9, 0.7, 0.7 Hz, 1H), 7.59−7.46 (m, 5H), 7.44 (d, J = 8.9 Hz, 1H), 7.37−7.31 (m, 2H), 7.25 (ddd, J = 8.4, 7.0, 1.4 Hz, 1H), 7.24 (ddd, J = 8.4, 7.0, 1.4 Hz, 1H), 2.54 (s, 3H). ^{13}C NMR (101 MHz, CD_2Cl_2, ppm) δ 140.8, 138.4, 132.4, 132.1, 131.79, 131.75, 131.42, 131.35, 131.2, 131.1, 130.4, 129.8, 129.7, 128.9, 128.8, 128.0, 127.9, 127.8, 127.6, 127.1, 126.9, 126.5, 126.4, 125.8, 125.0, 124.90, 124.86, 122.9, 17.52. MALDI-ToF MS (m/z) calcd for $C_{29}H_{20}$ 368.16, found 368.08 ($[M]^+$). MALDI-ToF HRMS (m/z) calcd for $C_{29}H_{20}^+$ 368.1560, found 368.1559 (|Δ| = 0.1 ppm).

*(±)-1,6-Dibromo-3-methyl-4-phenyldibenzo[c,g]phenanthrene (**34**).* A solution of bromine (0.67 mL, 13 mmol) in CH_2Cl_2 (10 mL) was added dropwise to a cooled (−78 °C) solution of **11** (2.08 g, 5.64 mmol) in CH_2Cl_2 (120 mL). The reaction mixture was allowed to warm to room temperature overnight and then it was stirred at room temperature for 2 d before saturated aqueous $Na_2S_2O_3$ was added to quench the excess of bromine. The organic layer was separated, washed with water and brine, dried over anhydrous Na_2SO_4, and filtered. After evaporation of the solvents, the residue was purified by column chromatography over silica gel using cyclohexane as an eluent to afford the desired product (2.79 g, 94%) as a pale yellow solid. ^{1}H NMR (500 MHz, CD_2Cl_2, ppm) δ 8.51 (s, 1H), 8.41 (ddd, J = 8.4, 1.4, 0.6 Hz, 1H), 8.33 (ddd, J = 8.3, 1.3, 0.6 Hz, 1H), 8.28 (dddd, J = 8.5, 1.2, 0.6, 0.6 Hz, 1H), 8.24 (dddd, J = 8.5, 1.2, 0.7, 0.7 Hz, 1H), 7.73 (s, 1H), 7.63 (ddd, J = 8.4, 6.9, 1.2 Hz, 1H), 7.59 (ddd, J = 8.2, 6.9, 1.3 Hz, 1H), 7.60−7.56 (m, 2H), 7.56−7.51 (m, 1H), 7.35−7.26 (m, 4H), 2.50 (s, 3H). ^{13}C NMR (101 MHz, CD_2Cl_2, ppm) δ 139.6, 138.3, 132.3, 132.2, 132.1, 131.6, 131.3, 130.6, 130.3 (two overlapped signals), 130.1, 130.0, 129.2, 129.0, 128.6, 128.1, 127.9, 127.7, 127.17, 127.15, 126.8, 126.6, 125.96, 125.95, 125.6 (two overlapped signals), 122.8, 122.2, 17.5. MALDI-ToF MS (m/z) calcd for $C_{29}H_{18}Br_2$ 523.98, found 524.39 ($[M]^+$). MALDI-ToF HRMS (m/z) calcd for $C_{29}H_{18}Br_2^+$ 523.9770, found 523.9768 (|Δ| = 0.3 ppm).

*(±)-3-Methyl-1,4,6-triphenyldibenzo[c,g]phenanthrene (**12**).* A mixture of **34** (2.81 g, 5.34 mmol), phenylboronic acid (2.60 g, 21.4 mmol), K_2CO_3 (7.38 g, 53.4 mmol), $Pd(PPh_3)_4$ (0.31 g, 0.27 mmol), and toluene/EtOH/water (210 mL, 4:2:1) was heated at 90 °C overnight under an argon atmosphere before aqueous HCl (25 mL, 2 M) was added to quench the reaction. The reaction mixture was extracted with CH_2Cl_2 (3 × 25 mL) and the combined organic layers were washed with brine, dried over anhydrous Na_2SO_4, and filtered. After evaporation of the solvents, the residue was purified by column chromatography over silica gel using cyclohexane as an eluent to afford the desired product (2.58 g, 92%) as a white solid. ^{1}H NMR (400 MHz, CD_2Cl_2, ppm) δ 8.54 (dddd, J = 8.5, 1.3, 0.6, 0.6 Hz, 1H), 8.49 (dddd, J = 8.5, 1.3, 0.6, 0.6 Hz, 1H), 8.16 (s, 1H), 8.00 (ddd, J = 8.3, 1.4, 0.6 Hz, 1H), 7.92 (ddd, J = 8.3, 1.4, 0.6 Hz, 1H), 7.77−7.74 (m, 2H), 7.63−7.39 (m, 15H), 7.34−7.25 (m, 3H), 2.56 (s, 3H). ^{13}C NMR (101 MHz, CD_2Cl_2, ppm) δ (two signals could not be detected

DOI: 10.1021/acs.joc.6b02246
J. Org. Chem. 2016, 81, 12303−12317

because of the signal overlap) 141.3, 141.1, 140.6, 139.7, 138.9, 138.7, 131.8, 131.7, 131.4, 131.29, 131.27, 131.1, 130.9, 130.6, 130.5, 130.3, 130.2, 130.1, 129.0, 128.9, 128.76, 128.75, 127.9, 127.7, 126.6, 126.41, 126.36, 126.34, 126.26, 125.4, 125.3, 124.90, 124.88, 123.4, 17.6. MALDI-ToF MS (m/z) calcd for $C_{41}H_{28}$ 520.22, found 521.67 ($[M + H]^+$). MALDI-ToF HRMS (m/z) calcd for $C_{41}H_{28}^+$ 520.2186, found 520.2184 ($|\Delta|$ = 0.3 ppm).

*(±)-3-(Bromomethyl)-1,4,6-triphenyldibenzo[c,g]phenanthrene (**35**).* A mixture of **12** (2.50 g, 4.56 mmol), *N*-bromosuccinimide (1.06 g, 5.93 mmol), dibenzoyl peroxide (55 mg, 0.23 mmol), and CCl_4 (160 mL) was heated at reflux overnight under an argon atmosphere before the solvent was evaporated and the residue was purified by column chromatography over silica gel using cyclohexane/CH_2Cl_2 (95:5 to 9:1) as an eluent to afford the desired product (2.43 g, 89%) as a pale yellow solid. ^{1}H NMR (400 MHz, $CDCl_3$, ppm) δ 8.54 (dddd, J = 8.5, 1.3, 0.6, 0.6 Hz, 1H), 8.54 (dddd, J = 8.5, 1.3, 0.6, 0.6 Hz, 1H), 8.24 (s, 1H), 8.03 (ddd, J = 8.3, 1.4, 0.6 Hz, 1H), 7.92 (ddd, J = 8.3, 1.4, 0.6 Hz, 1H), 7.80−7.77 (m, 2H), 7.64−7.39 (m, 16H), 7.30 (ddd, J = 8.5, 6.9, 1.6 Hz, 1H), 7.29 (ddd, J = 8.7, 7.0, 1.7 Hz, 1H), 4.88 (d, J = 10.4 Hz, 1H), 4.83 (d, J = 10.5 Hz, 1H). ^{13}C NMR (101 MHz, $CDCl_3$, ppm) δ (one signal could not be detected because of the signal overlap) 140.8, 140.6, 140.0, 139.8, 139.1, 138.3, 131.7, 131.32, 131.28, 131.1, 130.8, 130.6, 130.3, 130.2, 130.14, 130.06, 129.8, 129.2, 128.8, 128.72, 128.65, 128.6, 128.2, 127.8, 127.5, 127.3, 127.0, 126.9, 126.8, 126.3, 126.2, 125.1, 124.90, 124.86, 122.7, 30.5. MALDI-ToF MS (m/z) calcd for $C_{41}H_{27}Br$ 598.13, found 519.44 ($[M - Br]^+$).

*(±)-Methyl 3,3-dimethyl-2-((1,4,6-triphenyldibenzo[c,g]-phenanthren-3-yl)methyl)butanoate (**13**).* A solution of LDA (6.25 mL, 12.5 mmol, 2 M in THF/heptane) was added dropwise to a cooled (−78 °C) solution of methyl *tert*-butylacetate (1.95 g, 12.5 mmol) in dry THF (60 mL) under an argon atmosphere. The reaction mixture was stirred at −78 °C for 2 h before a suspension of **35** (500 mg, 0.833 mmol) in dry THF (30 mL) was added dropwise at −78 °C. The reaction was then allowed to warm to room temperature overnight before saturated aqueous NH_4Cl (25 mL) was added to quench the reaction. The reaction mixture was extracted with CH_2Cl_2 (3 × 25 mL) and the combined organic layers were washed with brine, dried over anhydrous Na_2SO_4, and filtered. After evaporation of the solvents, the residue was purified by column chromatography over silica gel using cyclohexane/CH_2Cl_2 (95:5 to 7:3) as an eluent to afford the desired product (360 mg, 67%) as a pale brown solid and as an approximately 1:1 mixture of two possible diastereomers. ^{1}H NMR (400 MHz, CD_2Cl_2, ppm) δ 8.48 (dddd, J = 8.5, 1.3, 0.6, 0.6 Hz, 1H), 8.48 (dddd, J = 8.6, 1.3, 0.7, 0.7 Hz, 1H), 8.47 (dddd, J = 8.6, 1.3, 0.7, 0.7 Hz, 1H), 8.47 (dddd, J = 8.8, 1.4, 0.7, 0.7 Hz, 1H), 8.29 (s, 1H), 8.26 (s, 1H), 8.02 (ddd, J = 8.3, 1.4, 0.6 Hz, 1H), 7.98 (ddd, J = 8.4, 1.4, 0.6 Hz, 1H), 7.93−7.88 (m, 4H), 7.79−7.74 (m, 2H), 7.65−7.38 (m, 30H), 7.36−7.32 (m, 1H), 7.32 (s, 1H), 7.29−7.23 (m, 4H), 3.64 (dd, J = 13.9, 11.8 Hz, 1H), 3.53 (dd, J = 13.9, 12.0 Hz, 1H), 3.29 (dd, J = 13.9, 3.3 Hz, 1H), 3.22 (dd, J = 14.1, 3.3 Hz, 1H), 3.09 (s, 3H), 2.88 (s, 3H), 2.50 (dd, J = 12.0, 3.3 Hz, 1H), 2.36 (dd, J = 11.9, 3.2 Hz, 1H), 0.78 (s, 9H), 0.71 (s, 9H). ^{13}C NMR (101 MHz, CD_2Cl_2, ppm) δ (out of 84 signals expected for two possible diastereomers, three signals could not be detected within the resolution limits of the NMR technique because of the signal overlap) 175.3, 175.2, 141.4, 141.2, 141.09, 141.07, 139.66, 139.65, 139.62, 139.59, 139.1, 139.0, 138.8, 138.6, 134.4, 133.7, 132.6, 132.0, 131.81, 131.75, 131.6, 131.4, 131.2, 131.1, 131.01, 131.00, 130.97, 130.95, 130.7, 130.6, 130.53, 130.52, 130.49, 130.44, 130.37, 130.29, 130.27, 130.26, 130.2, 129.4, 129.0, 128.88, 128.85, 128.78, 128.76, 128.0, 127.9, 127.82, 127.77, 127.70, 127.69, 126.68, 126.66, 126.64, 126.61, 126.57, 126.5, 126.33, 126.32, 126.2, 126.1, 125.8, 125.6, 125.2, 125.1, 125.0, 124.9, 124.79, 124.77, 124.1, 123.6, 57.2, 56.4, 50.9, 50.7, 33.5, 33.4, 28.0, 27.4, 27.24, 27.21. MALDI-ToF MS (m/z) calcd for $C_{48}H_{40}O_2$ 648.30, found 648.13 ($[M]^+$). MALDI-ToF HRMS (m/z) calcd for $C_{48}H_{40}O_2^+$ 648.3023, found 648.3021 ($|\Delta|$ = 0.3 ppm).

*(±)-3,3-Dimethyl-2-((1,4,6-triphenyldibenzo[c,g]phenanthren-3-yl)methyl)butanoic acid (**36**).* A mixture of **13** (200 mg, 0.308 mmol), lithium iodide (289 mg, 2.16 mmol), and 2,4,6-collidine (5 mL) was heated at 185 °C for 3 h under an argon atmosphere before the reaction mixture was cooled to room temperature and concentrated in a vacuum. To the residue, aqueous HCl (15 mL, 2 M) was added, and the precipitate that formed was filtered and washed with water to afford the desired product (158 mg, 81%) as a pale yellow solid and as an approximately 1:0.7 mixture of two possible diastereomers, which was used in the next step without further purification. ^{1}H NMR (400 MHz, CD_2Cl_2, ppm) δ 8.50−8.41 (m, 3.3H), 8.38 (s, 1H), 8.30 (s, 0.7H), 8.00 (d, J = 8.3 Hz, 0.7H), 7.96 (d, J = 8.3 Hz, 1H), 7.90 (d, J = 8.1 Hz, 1H), 7.89 (d, J = 7.9 Hz, 0.7H), 7.84−7.79 (m, 1.3H), 7.73−7.69 (m, 2H), 7.64−7.37 (m, 25H) 7.35−7.30 (m, 1.7H), 7.29−7.21 (m, 3.3H), 3.65 (dd, J = 14.2, 12.4 Hz, 1H), 3.51 (dd, J = 13.7, 12.1 Hz, 0.7H), 3.31 (dd, J = 14.0, 3.4 Hz, 0.7H), 3.21 (dd, J = 14.1, 3.5 Hz, 1H), 2.59 (dd, J = 11.6, 3.1 Hz, 0.7H), 2.45 (dd, J = 12.1, 3.4 Hz, 1H). MALDI-ToF MS (m/z) calcd for $C_{47}H_{38}O_2$ 634.29, found 634.27 ($[M]^+$).

*(±)-5-(tert-Butyl)-1,3,7-triphenyl-4,5-dihydro-6H-naphtho[3,2,1-no]tetraphen-6-one (**14**).* A solution of **36** (158 mg, 0.244 mmol) in oxalyl chloride (15 mL) was heated at reflux for 2.5 h before the excess of oxalyl chloride was removed under the reduced pressure. The crude acid chloride intermediate was dissolved in CH_2Cl_2 (20 mL) and the solution was cooled to −78 °C. Solid $AlCl_3$ (97 mg, 0.73 mmol) was added and the reaction mixture was allowed to warm to −10 °C over 5 h before it was poured onto ice and acidified with aqueous HCl (2 M). The organic layer was separated and the aqueous layer was extracted with CH_2Cl_2. The combined organic layers were washed with saturated aqueous $NaHCO_3$, water, and brine, dried over anhydrous Na_2SO_4, and filtered. After evaporation of the solvents, the residue was purified by column chromatography over silica gel using cyclohexane/CH_2Cl_2 (4:1 to 5:2) as an eluent to afford the desired product (115 mg, 77%) as a pale yellow solid and as an approximately 1:0.4 mixture of two possible diastereomers. ^{1}H NMR (400 MHz, CD_2Cl_2, ppm) δ 8.51 (dddd, J = 8.5, 1.3, 0.7, 0.7 Hz, 1H), 8.50 (dddd, J = 8.5, 1.3, 0.6, 0.6 Hz, 0.4H), 8.43 (dddd, J = 8.5, 1.3, 0.6, 0.6 Hz, 1H), 8.35 (dddd, J = 8.5, 1.3, 0.6, 0.6 Hz, 0.4H), 7.92 (d, J = 8.4 Hz, 1.4H), 7.65−7.22 (m, 29.4H), 3.38 (dd, J = 16.5, 5.6 Hz, 1H), 3.26 (dd, J = 16.9, 6.0 Hz, 0.4H), 3.16 (dd, J = 16.9, 7.6 Hz, 0.4H), 3.08 (dd, J = 16.6, 10.0 Hz, 1H), 2.92 (dd, J = 10.0, 5.6 Hz, 1H), 2.66 (dd, J = 7.5, 6.0 Hz, 0.4H), 0.88 (s, 9H), 0.85 (s, 3.6H). ^{13}C NMR (101 MHz, CD_2Cl_2, ppm) δ (out of 86 signals expected for two possible diastereomers, 13 signals could not be detected within the resolution limits of the NMR technique because of the signal overlap) 203.6, 202.8, 140.91, 140.89, 140.3, 140.2, 139.72, 139.71, 139.6, 139.47, 139.46, 138.8, 137.7, 137.6, 132.8, 132.6, 132.4, 132.3, 131.8, 131.73, 131.72, 131.4, 131.3, 131.22, 131.15, 131.02, 130.99, 130.96, 130.6, 130.5, 130.4, 130.3, 130.1, 130.0, 129.9, 129.84, 129.83, 129.78, 129.76, 129.33, 129.27, 129.1, 128.8, 128.60, 128.55, 128.4, 128.3, 128.09, 128.06, 127.8, 127.4, 127.3, 127.0, 126.9, 126.8, 126.7, 126.5, 126.4, 126.34, 126.32, 125.7, 125.5, 125.1, 125.0, 124.8, 59.4, 58.5, 33.6, 32.9, 31.9, 31.1, 28.1, 27.8. MALDI-ToF MS (m/z) calcd for $C_{47}H_{36}O$ 616.28, found 616.07 ($[M]^+$). MALDI-ToF HRMS (m/z) calcd for $C_{47}H_{36}O^+$ 616.2761, found 616.2760 ($|\Delta|$ = 0.1 ppm).

*(±)-5-(tert-Butyl)-1,3,7-triphenyl-5,6-dihydro-4H-naphtho[3,2,1-no]tetraphen-6-ol (**37**).* A mixture of **14** (100 mg, 0.162 mmol), $LiAlH_4$ (118 mg, 0.486 mmol), and dry THF (10 mL) was stirred at room temperature for 10 min under an argon atmosphere before the reaction was quenched by the addition of ice and aqueous HCl (10 mL, 2 M). The organic layer was separated and the aqueous layer was extracted with CH_2Cl_2. The combined organic layers were washed with brine, dried over anhydrous Na_2SO_4, and filtered. After evaporation of the solvents, the residue was purified by column chromatography over silica gel using cyclohexane/CH_2Cl_2 (1:1) as an eluent to afford the desired product (67 mg, 67%) as a pale brown solid and as an approximately 1:0.8 mixture of two out of four possible diastereomers. ^{1}H NMR (400 MHz, CD_2Cl_2, ppm) δ 8.52−8.44 (m, 2.8H), 8.37 (dd, J = 8.5, 1.1 Hz, 0.8H), 7.94−7.88 (m, 1.8H), 7.67−7.30 (m, 34.2H), 7.28−7.19 (m, 3.6H), 5.31−5.29 (m, 1H), 5.24−5.20 (m, 0.8H), 3.13 (dd, J = 16.2, 13.4 Hz, 0.8H), 3.08 (dd, J = 16.5, 13.3 Hz, 1H), 2.89 (ddd, J = 16.4, 4.2, 1.2 Hz, 1H), 2.72 (ddd, J = 16.2, 3.3, 1.4 Hz, 0.8H), 1.80 (ddd, J = 13.2, 4.1, 1.5 Hz, 1H), 1.69 (ddd, J = 13.3, 3.2, 1.8 Hz, 0.8H), 0.88 (s, 9H), 0.87 (s, 7.2H). ^{13}C NMR (101

DOI: 10.1021/acs.joc.6b02246
J. Org. Chem. 2016, 81, 12303−12317

MHz, CD_2Cl_2, ppm) δ (out of 86 signals expected for two possible diastereomers, four signals could not be detected within the resolution limits of the NMR technique because of the signal overlap) 141.1, 141.0, 140.1, 139.7, 139.2, 139.07, 139.05, 139.0, 138.1, 137.8, 137.5, 136.2, 134.9, 134.8, 134.1, 133.6, 132.5, 132.1, 132.0, 131.8, 131.4, 131.3, 131.24, 131.21, 131.1, 131.01, 130.97, 130.92, 130.85, 130.83, 130.76, 130.5, 130.4, 130.3, 130.1, 130.0, 129.94, 129.88, 129.8, 129.2, 129.1, 129.04, 129.02, 128.99, 128.9, 128.78, 128.76, 128.7, 128.6, 128.1, 128.0, 127.9, 127.8, 127.73, 127.70, 127.69, 127.4, 127.3, 127.2, 126.8, 126.6, 126.5, 126.42, 126.37, 125.4, 125.3, 125.1, 124.90, 124.88, 124.84, 124.75, 124.7, 67.5, 67.3, 49.0, 48.8, 33.0, 32.8, 28.5, 28.4, 25.3, 24.9. MALDI-ToF MS (m/z) calcd for $C_{47}H_{38}O$ 618.29, found 618.23 ($[M]^+$). MALDI-ToF HRMS (m/z) calcd for $C_{47}H_{38}O^+$ 618.2917, found 618.2916 ($|\Delta|$ = 0.2 ppm).

*(±)-5-(tert-Butyl)-1,3,7-triphenyl-4H-naphtho[3,2,1-no]-tetraphene (**15**).* *p*-Toluenesulfonic acid monohydrate (2.6 mg, 0.014 mmol) was added to a hot (90 °C) solution of **37** (28 mg, 0.045 mmol) in toluene (5 mL) and the reaction mixture was heated at 90 °C for 5 min before it was cooled in an ice bath and passed through a pad of silica gel using toluene as an eluent to afford the desired product (24 mg, 88%) as a pale yellow solid. ^{1}H NMR (600 MHz, C_6D_6, ppm) δ 8.90 (dddd, J = 8.6, 1.3, 0.6, 0.6 Hz, 1H), 8.79 (dddd, J = 8.4, 1.3, 0.6, 0.6 Hz, 1H), 8.11 (ddd, J = 8.3, 1.4, 0.5 Hz, 1H), 7.77 (s, 1H), 7.74 (ddd, J = 8.4, 1.3, 0.6 Hz, 1H), 7.58−7.55 (m, 2H), 7.53 (d, J = 7.5 Hz, 1H), 7.47 (d, J = 7.5 Hz, 1H), 7.36 (dd, J = 7.8, 7.8 Hz, 1H), 7.35 (dd, J = 7.8, 7.7 Hz, 1H), 7.31 (dddd, J = 7.6, 7.4, 1.5, 0.7 Hz, 1H), 7.27 (dddd, J = 7.5, 7.5, 1.3, 1.3 Hz, 1H), 7.24−7.11 (m, 9H), 7.09 (ddd, J = 8.3, 6.8, 1.4 Hz, 1H), 7.01 (ddd, J = 8.3, 6.8, 1.3 Hz, 1H), 6.77 (dd, J = 1.6, 1.6 Hz, 1H), 3.79 (dd, J = 23.9, 1.4 Hz, 1H), 3.75 (dd, J = 23.8, 1.9 Hz, 1H), 0.91 (s, 9H). ^{13}C NMR (101 MHz, C_6D_6, ppm) δ 147.5, 141.3, 140.1, 140.0, 139.5, 137.4, 134.2, 133.6, 132.43, 132.39, 131.9, 131.5, 131.3, 131.21, 131.16, 130.4, 130.3 (two overlapped signals), 130.2, 129.8, 129.6, 129.3, 129.00, 128.97, 128.8, 128.6, 128.4, 127.7, 127.5 (two overlapped signals), 127.2, 127.0, 126.9, 126.7 (two overlapped signals), 125.9, 125.04, 124.95, 124.3, 118.6, 35.7, 31.5, 28.8. MALDI-ToF MS (m/z) calcd for $C_{47}H_{36}$ 600.28, found 600.34 ($[M]^+$). MALDI-ToF HRMS (m/z) calcd for $C_{47}H_{36}^+$ 600.2812, found 600.2819 ($|\Delta|$ = 1.3 ppm).

Single-Crystal X-ray Diffraction (XRD). Single crystals of compounds **15** and **29** suitable for X-ray diffraction analysis were grown from the corresponding solutions in CH_2Cl_2 by slow evaporation of the solvent. Data collections for both crystal structures were performed at low temperatures (123 K) using Ga Kα radiation on a STOE STADIVARI diffractometer equipped with a Metaljet D2 generator, AXO ASTIX++ multilayer mirrors and a Pilatus 3R 300 K detector. Integration of the frames and data reduction was carried out using the STOE X-Area software.[19] The structures were solved by the charge-flipping method using Superflip.[20] All non-hydrogen atoms were refined anisotropically by full-matrix least-squares on F using CRYSTALS.[21] The crystallographic views of the solid-state structures of **15** and **29** are shown in Figure S23. The crystal parameters and structure refinements for **15** and **29** are summarized below and in Table S3. The crystallographic parameters were deposited into the Cambridge Crystallographic Data Centre (CCDC).

*Compound **15**.* $C_{47}H_{36}$; 0.01 × 0.09 × 0.16 mm; monoclinic, $C2/c$ (No. 15); a = 26.5471(7), b = 10.0841(3), and c = 27.9848(8) Å; α = 90, β = 119.013(2), and γ = 90°; V = 6551.5(3) Å^3; Z = 8; T = 123 K; ρ_{calc} = 1.218 g cm^{-3}; μ = 0.330 mm^{-1}. CCDC no.: 1487740.

*Compound **29**.* $C_{29}H_{22}O$; 0.02 × 0.03 × 0.15 mm; orthorhombic, $P2_12_12_1$ (No. 19); a = 6.3779(3), b = 19.3600(8), and c = 31.3111(12) Å; α = 90, β = 90, and γ = 90°; V = 3866.2(3) Å^3; Z = 8; T = 123 K; ρ_{calc} = 1.328 g cm^{-3}; μ = 0.385 mm^{-1}. CCDC no.: 1487741.

Nuclear Magnetic Resonance (NMR) Spectroscopy. The isomerization of **9a** to **9b** was followed (Figure S1) by ^{1}H NMR spectroscopy (400 MHz, CD_2Cl_2, 25 °C). This isomerization process occurs spontaneously in deuterated solvents that contain trace amounts of acids, such as CD_2Cl_2, during an NMR experiment, or it can be performed on a larger scale by using trifluoroacetic acid, which instantly converts **9a** to **9b**. The structures of both compounds were confirmed by 2D NMR spectroscopy (see Sections S9 and S10).

The σ-dimer-formation process of **5b** was followed by 1D and 2D NMR spectroscopy (400, 600, and 700 MHz, C_6D_6). The radical species **5b** were generated from the hydro-precursors **9a** or **9b** by oxidation with *p*-chloranil (CA). The 1D and 2D NMR measurements revealed that **5b** is in equilibrium with its σ-dimers **16a** and **16b** and undergoes slow oxidation to afford keto-compounds **17a** and **17b** as two major final products (Figures S2 and S3). Presumably, the oxidation occurs on account of trace amounts of oxygen present in the argon-saturated sample. Additionally, intermediate species **38** and **39** (Figure S12) that form over the course of the reaction were identified. The use of either **9a** or **9b** in this reaction gave similar results (Figures S2 and S3), as oxidation with CA generates the same radical species **5b**. In the case when **9a** was used, small amounts of **9b** were observed (Figure S2) as the reaction progressed. The isomerization of **9a** to **9b** was most likely catalyzed by reduced CA species containing phenolic hydroxyl groups that are acidic. The structures of the final products **17a** and **17b** were confirmed by 2D NMR spectroscopy once the reaction was completed, that is, when the starting material **9b** and the σ-dimers **16** were not present anymore. The combination of TOCSY and NOESY, as well as high-resolution HSQC and HMBC NMR techniques (600 MHz, C_6D_6, 25 °C) allowed for unambiguous structural validation of both **17a** (Figures S4 and S6−S8) and **17b** (Figures S5 and S9−S11). The structures of the relatively short-lived intermediate species **16a**, **16b**, **38**, and **39** were confirmed during an NMR experiment at a lower temperature (15 °C), at which these compounds exhibited a prolonged lifetime of approximately 1 day. The combination of TOCSY, NOESY, and PFGSE, as well as high-resolution HSQC and HMBC NMR techniques (700 MHz, C_6D_6, 15 °C) allowed for structural validation of all four compounds that were present in the reaction mixture together with the starting material **9a** and/or **9b**, the final products **17a** and **17b**, and small amounts of other unidentified species. The characteristic proton resonances of **16a**, **16b**, **38**, and **39** are highlighted in Figure S12 and all their carbon resonances that could be identified are highlighted in Figure S13. Assignment of the proton and carbon resonances to the corresponding atoms is shown in Figures S14 (**16a**), S15 (**16b**), S16 (**38**), and S17 (**39**). All acquired spectra used for identification of compounds **16a**, **16b**, **38**, and **39** were submitted as a separate Supporting Information zip file. Proton and carbon resonances of the phenyl group could not be assigned for compounds **16a**, **16b**, **17b**, **38**, and **39** because of signal overlap.

Diffusion coefficients (D) obtained from the PFGSE NMR experiments for **9a** (1.088×10^{-9} m^2 s^{-1}), **16a** (8.250×10^{-8} m^2 s^{-1}), **16b** (8.029×10^{-8} m^2 s^{-1}), **38** (1.085×10^{-8} m^2 s^{-1}), and **39** (9.222×10^{-8} m^2 s^{-1}) were used to estimate the ratio between the molecular weight of **16a**, **16b**, **38**, and **39** and the molecular weight of **9a**, which was in all cases in a good qualitative agreement with the calculated value (in the brackets): **16a**/2.3 (2), **16b**/2.5 (2), **38**/1 (1.1), and **39**/1.2 (1.5).

Sample Preparation for the σ-Dimer-Formation NMR Experiments. Stock solutions of the starting material, **9a** or **9b**, and CA were saturated with argon by using the freeze−pump−thaw technique in three cycles. The NMR spectra were acquired before and after the addition of the solution of CA to the solution of **9a** or **9b**. After the addition of CA, the NMR tube was sealed.

Electron Paramagnetic Resonance (EPR) Spectroscopy. Compound **5b** was generated in situ by oxidation of either **9a** or **9b** with CA in an argon-saturated toluene at 25 °C, and the reaction was monitored by electron paramagnetic resonance (EPR) spectroscopy in solution. Compound **5c** was generated in situ by heating a mixture of **15** and 1 equiv of CA in an argon-saturated toluene for 3 h at 65 °C. Subsequently, the EPR spectrum was recorded at variable temperatures. The spin concentration was determined by calibration with TEMPO.

Circular Dichroism (CD) Spectroscopy. The enantiomers of **15**, (*P*)-**15** and (*M*)-**15**, obtained from chiral-stationary-phase HPLC (multiple fractions were combined) were each dissolved in *tert*-butyl methyl ether and the solutions were saturated with argon. To these solutions, an argon-saturated solution of CA (10 equiv with respect to **15**) was added and the CD spectra were recorded at 25 °C.

DOI: 10.1021/acs.joc.6b02246
J. Org. Chem. 2016, 81, 12303−12317

Theoretical Calculations. All DFT calculations were performed in Gaussian 09 (Revision D.01) suite of electronic structure programs. Geometries were optimized using (U)B3LYP functional and 6-31G(d,p) basis set in the gas phase. Chemcraft software was used to analyze the TD-DFT calculated spectra and to generate graphical images of frontier molecular orbitals (FMOs). The nucleus independent chemical shift (NICS) calculations were performed on UB3LYP/6-31G(d,p) optimized geometry at the GIAO-UB3LYP/6-31G(d,p) level. Considering the nonplanarity of the molecule, NICS(1) values were obtained by placing dummy atoms 1 Å above and below each benzenoid ring.

■ ASSOCIATED CONTENT

Supporting Information

The Supporting Information is available free of charge on the ACS Publications website at DOI: 10.1021/acs.joc.6b02246.

Detailed synthetic schemes, spectroscopic (NMR, EPR), kinetic (CD), computational (DFT), and crystallographic data, copies of ^{1}H and ^{13}C NMR, and MALDI-ToF MS spectra, and Cartesian coordinates for all optimized geometries (PDF)
Crystal data (CIF)
Crystal data (CIF)
NMR data (ZIP)
MOL2 data (ZIP)

■ AUTHOR INFORMATION

Corresponding Author

*Phone: +41 61 207 10 15. Fax: +41 61 267 09 76. E-mail: michal.juricek@unibas.ch.

Notes

The authors declare no competing financial interest.

■ ACKNOWLEDGMENTS

We would like to thank Prof. Dr. Marcel Mayor for generously hosting our group at the University of Basel and his invaluable support of our research. The Swiss National Science Foundation (SNSF, M.J./PZ00P2_148043 and D.H./200021_130263) and the Novartis University of Basel Excellence Scholarship for Life Sciences (P.R. and M.J.) are gratefully acknowledged for their financial support.

■ REFERENCES

(1) (a) Konishi, A.; Kubo, T. In *Chemical Science of π-Electron Systems*; Akasaka, T., Osuka, A., Fukuzumi, S., Kandori, H., Aso, Y., Eds.; Springer: Tokyo, Japan, 2015; pp 337−360. (b) Kubo, T. *Chem. Rec.* **2015**, *15*, 218−232. (c) Sun, Z.; Zeng, Z.; Wu, J. *Acc. Chem. Res.* **2014**, *47*, 2582−2591. (d) Morita, Y.; Suzuki, S.; Sato, K.; Takui, T. *Nat. Chem.* **2011**, *3*, 197−204. (e) Morita, Y.; Nishida, S. In *Stable Radicals: Fundamentals and Applied Aspects of Odd-Electron Compounds*; Hicks, R. G., Ed.; John Wiley & Sons, Ltd.: Wiltshire, U.K., 2010; pp 81−145.

(2) (a) O'Connor, G. D.; Troy, T. P.; Roberts, D. A.; Chalyavi, N.; Fückel, B.; Crossley, M. J.; Nauta, K.; Stanton, J. F.; Schmidt, T. W. *J. Am. Chem. Soc.* **2011**, *133*, 14554−14557. (b) Reid, D. H. *Q. Rev., Chem. Soc.* **1965**, *19*, 274−302. (c) Sogo, P. B.; Nakazaki, M.; Calvin, M. *J. Chem. Phys.* **1957**, *26*, 1343−1345.

(3) (a) Shimizu, A.; Kubo, T.; Uruichi, M.; Yakushi, K.; Nakano, M.; Shiomi, D.; Sato, K.; Takui, T.; Hirao, Y.; Matsumoto, K.; Kurata, H.; Morita, Y.; Nakasuji, K. *J. Am. Chem. Soc.* **2010**, *132*, 14421−14428. (b) Shimizu, A.; Uruichi, M.; Yakushi, K.; Matsuzaki, H.; Okamoto, H.; Nakano, M.; Hirao, Y.; Matsumoto, K.; Kurata, H.; Kubo, T. *Angew. Chem., Int. Ed.* **2009**, *48*, 5482−5486. (c) Huang, J.; Kertesz, M. *J. Am. Chem. Soc.* **2007**, *129*, 1634−1643. (d) Kubo, T.; Shimizu, A.; Sakamoto, M.; Uruichi, M.; Yakushi, K.; Nakano, M.; Shiomi, D.; Sato, K.; Takui, T.; Morita, Y.; Nakasuji, K. *Angew. Chem., Int. Ed.* **2005**, *44*, 6564−6568. (e) Goto, K.; Kubo, T.; Yamamoto, K.; Nakasuji, K.; Sato, K.; Shiomi, D.; Takui, T.; Kubota, M.; Kobayashi, T.; Yakusi, K.; Ouyang, J. Y. *J. Am. Chem. Soc.* **1999**, *121*, 1619−1620.

(4) (a) Cui, Z.-H.; Lischka, H.; Beneberu, H. Z.; Kertesz, M. *J. Am. Chem. Soc.* **2014**, *136*, 5539−5542. (b) Mou, Z.; Uchida, K.; Kubo, T.; Kertesz, M. *J. Am. Chem. Soc.* **2014**, *136*, 18009−18022. (c) Cui, Z.-H.; Lischka, H.; Beneberu, H. Z.; Kertesz, M. *J. Am. Chem. Soc.* **2014**, *136*, 12958−12965. (d) Tian, Y.-H.; Huang, J.; Kertesz, M. *Phys. Chem. Chem. Phys.* **2010**, *12*, 5084−5093. (e) Suzuki, S.; Morita, Y.; Fukui, K.; Sato, K.; Shiomi, D.; Takui, T.; Nakasuji, K. *J. Am. Chem. Soc.* **2006**, *128*, 2530−2531. (f) Takano, Y.; Taniguchi, T.; Isobe, H.; Kubo, T.; Morita, Y.; Yamamoto, K.; Nakasuji, K.; Takui, T.; Yamaguchi, K. *J. Am. Chem. Soc.* **2002**, *124*, 11122−11130.

(5) (a) Koike, H.; Chikamatsu, M.; Azumi, R.; Tsutsumi, J. Y.; Ogawa, K.; Yamane, W.; Nishiuchi, T.; Kubo, T.; Hasegawa, T.; Kanai, K. *Adv. Funct. Mater.* **2016**, *26*, 277−283. (b) Morita, Y.; Suzuki, S.; Fukui, K.; Nakazawa, S.; Kitagawa, H.; Kishida, H.; Okamoto, H.; Naito, A.; Sekine, A.; Ohashi, Y.; Shiro, M.; Sasaki, K.; Shiomi, D.; Sato, K.; Takui, T.; Nakasuji, K. *Nat. Mater.* **2008**, *7*, 48−51. (c) Chikamatsu, M.; Mikami, T.; Chisaka, J.; Yoshida, Y.; Azumi, R.; Yase, K.; Shimizu, A.; Kubo, T.; Morita, Y.; Nakasuji, K. *Appl. Phys. Lett.* **2007**, *91*, 043506. (d) Nishida, S.; Morita, Y.; Fukui, K.; Sato, K.; Shiomi, D.; Takui, T.; Nakasuji, K. *Angew. Chem., Int. Ed.* **2005**, *44*, 7277−7280.

(6) (a) Hicks, R. G. *Nat. Chem.* **2011**, *3*, 189−191. (b) Pal, S. K.; Bag, P.; Sarkar, A.; Chi, X.; Itkis, M. E.; Tham, F. S.; Donnadieu, B.; Haddon, R. C. *J. Am. Chem. Soc.* **2010**, *132*, 17258−17264. (c) Bag, P.; Itkis, M. E.; Pal, S. K.; Donnadieu, B.; Tham, F. S.; Park, H.; Schlueter, J. A.; Siegrist, T.; Haddon, R. C. *J. Am. Chem. Soc.* **2010**, *132*, 2684−2694. (d) Pal, S. K.; Itkis, M. E.; Tham, F. S.; Reed, R. W.; Oakley, R. T.; Donnadieu, B.; Haddon, R. C. *J. Am. Chem. Soc.* **2007**, *129*, 7163−7174. (e) Mandal, S. K.; Samanta, S.; Itkis, M. E.; Jensen, D. W.; Reed, R. W.; Oakley, R. T.; Tham, F. S.; Donnadieu, B.; Haddon, R. C. *J. Am. Chem. Soc.* **2006**, *128*, 1982−1994. (f) Itkis, M. E.; Chi, X.; Cordes, A. W.; Haddon, R. C. *Science* **2002**, *296*, 1443−1445. (g) Chi, X.; Itkis, M. E.; Kirschbaum, K.; Pinkerton, A. A.; Oakley, R. T.; Cordes, A. W.; Haddon, R. C. *J. Am. Chem. Soc.* **2001**, *123*, 4041−4048.

(7) Galán-Mascarós, J. R. *Nat. Phys.* **2015**, *11*, 7−8.

(8) For recent examples of the magnetochiral dichroism (MChD) effect, see: (a) Sessoli, R.; Boulon, M.-E.; Caneschi, A.; Mannini, M.; Poggini, L.; Wilhelm, F.; Rogalev, A. *Nat. Phys.* **2015**, *11*, 69−74. (b) Kitagawa, Y.; Segawa, H.; Ishii, K. *Angew. Chem., Int. Ed.* **2011**, *50*, 9133−9136. (c) Train, C.; Gheorghe, R.; Krstic, V.; Chamoreau, L.-M.; Ovanesyan, N. S.; Rikken, G. L. J. A.; Gruselle, M.; Verdaguer, M. *Nat. Mater.* **2008**, *7*, 729−734. (d) Rikken, G. L. J. A.; Raupach, E. *Nature* **1997**, *390*, 493−494. (e) Barron, L. D.; Vrbancich, J. *Mol. Phys.* **1984**, *51*, 715−730.

(9) For recent examples of the electrical magnetochiral anisotropy (eMChA) effect, see: (a) Pop, F.; Auban-Senzier, P.; Canadell, E.; Rikken, G. L. J. A.; Avarvari, N. *Nat. Commun.* **2014**, *5*, 3757. (b) Krstić, V.; Roth, S.; Burghard, M.; Kern, K.; Rikken, G. L. J. A. *J. Chem. Phys.* **2002**, *117*, 11315−11319. (c) Rikken, G. L. J. A.; Fölling, J.; Wyder, P. *Phys. Rev. Lett.* **2001**, *87*, 236602. For recent examples of the related chirality-induced spin selectivity (CISS) effect, see: (d) Naaman, R.; Waldeck, D. H. *J. Phys. Chem. Lett.* **2012**, *3*, 2178−2187. (e) Göhler, B.; Hamelbeck, V.; Markus, T. Z.; Kettner, M.; Hanne, G. F.; Vager, Z.; Naaman, R.; Zacharias, H. *Science* **2011**, *331*, 894−897.

(10) (a) Anamimoghadam, O.; Symes, M. D.; Long, D.-L.; Sproules, S.; Cronin, L.; Bucher, G. *J. Am. Chem. Soc.* **2015**, *137*, 14944−14951. (b) Ueda, A.; Wasa, H.; Suzuki, S.; Okada, K.; Sato, K.; Takui, T.; Morita, Y. *Angew. Chem., Int. Ed.* **2012**, *51*, 6691−6695. For recent examples of helical spin-delocalized open-shell (c) radical and (d) radical ion not based on phenalenyl, see: (c) Wang, Y.; Zhang, H.; Pink, M.; Olankitwanit, A.; Rajca, S.; Rajca, A. *J. Am. Chem. Soc.* **2016**, *138*, 7298−7304. (d) Zak, J. K.; Miyasaka, M.; Rajca, S.; Lapkowski, M.; Rajca, A. *J. Am. Chem. Soc.* **2010**, *132*, 3246−3247. For recent examples of helically chiral biradicaloids, featuring spin-delocalization

DOI: 10.1021/acs.joc.6b02246
J. Org. Chem. 2016, 81, 12303−12317

over a [5]helicene backbone in the triplet state, see: (e) Ravat, P.; Šolomek, T.; Ribar, P.; Juríček, M. *Synlett* **2016**, *27*, 1613−1617. (f) Ravat, P.; Šolomek, T.; Rickhaus, M.; Häussinger, D.; Neuburger, M.; Baumgarten, M.; Juríček, M. *Angew. Chem., Int. Ed.* **2016**, *55*, 1183−1186. (g) Liu, J.; Ravat, P.; Wagner, M.; Baumgarten, M.; Feng, X.; Müllen, K. *Angew. Chem., Int. Ed.* **2015**, *54*, 12442−12446.

(11) (a) Nishida, S.; Morita, Y.; Ueda, A.; Kobayashi, T.; Fukui, K.; Ogasawara, K.; Sato, K.; Takui, T.; Nakasuji, K. *J. Am. Chem. Soc.* **2008**, *130*, 14954−14954. For recent examples of neutral open-shell radicals not based on phenalenyl, in which spin-delocalization is extended partially over a curved backbone, see: (b) Ueda, A.; Nishida, S.; Fukui, K.; Ise, T.; Shiomi, D.; Sato, K.; Takui, T.; Nakasuji, K.; Morita, Y. *Angew. Chem., Int. Ed.* **2010**, *49*, 1678−1682. (c) Morita, Y.; Ueda, A.; Nishida, S.; Fukui, K.; Ise, T.; Shiomi, D.; Sato, K.; Takui, T.; Nakasuji, K. *Angew. Chem., Int. Ed.* **2008**, *47*, 2035−2038.

(12) Rickhaus, M.; Mayor, M.; Juríček, M. *Chem. Soc. Rev.* **2016**, *45*, 1542−1556.

(13) Goretta, S.; Tasciotti, C.; Mathieu, S.; Smet, M.; Maes, W.; Chabre, Y. M.; Dehaen, W.; Giasson, R.; Raimundo, J.-M.; Henry, C. R.; Barth, C.; Gingras, M. *Org. Lett.* **2009**, *11*, 3846−3849.

(14) (a) Broene, R. D.; Diederich, F. *Tetrahedron Lett.* **1991**, *32*, 5227−5230. (b) Logani, M. K.; Austin, W. A.; Davies, R. E. *Tetrahedron Lett.* **1977**, *18*, 2467−2470. (c) Sandin, R. B.; Fieser, L. F. *J. Am. Chem. Soc.* **1940**, *62*, 3098−3105. (d) Cook, J. W.; Martin, R. H. *J. Chem. Soc.* **1940**, 1125−1127. (e) Bachmann, W. E.; Chemerda, J. M. *J. Am. Chem. Soc.* **1939**, *61*, 2358−2361.

(15) Uchida, K.; Hirao, Y.; Kurata, H.; Kubo, T.; Hatano, S.; Inoue, K. *Chem. - Asian J.* **2014**, *9*, 1823−1829.

(16) Zaitsev, V.; Rosokha, S. V.; Head-Gordon, M.; Kochi, J. K. *J. Org. Chem.* **2006**, *71*, 520−526.

(17) Goedicke, C.; Stegemeyer, H. *Tetrahedron Lett.* **1970**, *11*, 937−940.

(18) Fulmer, G. R.; Miller, A. J. M.; Sherden, N. H.; Gottlieb, H. E.; Nudelman, A.; Stoltz, B. M.; Bercaw, J. E.; Goldberg, K. I. *Organometallics* **2010**, *29*, 2176−2179.

(19) *X-Area Software*; Stoe & Cie, 2011.

(20) Palatinus, L.; Chapuis, G. *J. Appl. Crystallogr.* **2007**, *40*, 786−790.

(21) Betteridge, P. W.; Carruthers, J. R.; Cooper, R. I.; Prout, K.; Watkin, D. J. *J. Appl. Crystallogr.* **2003**, *36*, 1487.

DOI: 10.1021/acs.joc.6b02246
J. Org. Chem. 2016, 81, 12303−12317